

AD-A062 770

ARMY ELECTRONICS RESEARCH AND DEVELOPMENT COMMAND WS--ETC F/G 14/2
HELICOPTER REMOTE WIND SENSOR FLIGHT TEST.(U)
FEB 80 D H DICKSON, J E OTTESEN

UNCLASSIFIED

ERADCOM/ASL-TR-0051

NL

1 OF 1
AD
1085770

END
DATE
FILMED
5-80
DTIC

LEVEL II

AD

Reports Control Symbol
OSD 1366

12

ASL-TR-0051

ADA 082770

HELICOPTER REMOTE WIND SENSOR FLIGHT TEST

FEBRUARY 1980

By

David H. Dickson

US Army Atmospheric Sciences Laboratory
White Sands Missile Range, New Mexico 88002

Jon E. Ottesen

Physical Science Laboratory
New Mexico State University
University Park, New Mexico 88003

DTIC
ELECTE

APR 8 1980

Approved for public release; distribution unlimited

E

US Army Electronics Research and Development Command
ATMOSPHERIC SCIENCES LABORATORY
White Sands Missile Range, NM 88002

80 4 7 152

DEPARTMENT OF THE ARMY
US ARMY ATMOSPHERIC SCIENCES LABORATORY
DELAS-DMA
WHITE SANDS MISSILE RANGE, NM 88002

OFFICIAL BUSINESS

POSTAGE AND FEES PAID
DEPARTMENT OF THE ARMY
DOD 314

DDC FILE COPY



NOTICES

Abolition

The following is the space in which to be considered as a notice of the abolition of the Army, Navy, and Air Force, and the abolition of the Air Force, and the abolition of the Air Force.

The following is the space in which to be considered as a notice of the abolition of the Air Force, and the abolition of the Air Force, and the abolition of the Air Force, and the abolition of the Air Force.

Abolition

The following is the space in which to be considered as a notice of the abolition of the Air Force, and the abolition of the Air Force, and the abolition of the Air Force, and the abolition of the Air Force.

REPORT DOCUMENTATION PAGE		READ INSTRUCTIONS BEFORE COMPLETING FORM
1. REPORT NUMBER ASL-TR-0051	2. GOVT ACCESSION NO.	3. RECIPIENT'S CATALOG NUMBER
4. TITLE (and Subtitle) HELICOPTER REMOTE WIND SENSOR FLIGHT TEST.		5. TYPE OF REPORT & PERIOD COVERED RAD Technical Reports
7. AUTHOR(s) David H. Dickson Jon E. Ottesen		6. PERFORMING ORG. REPORT NUMBER
9. PERFORMING ORGANIZATION NAME AND ADDRESS Atmospheric Sciences Laboratory White Sands Missile Range, New Mexico 88002		8. CONTRACT OR GRANT NUMBER(s) 11531
11. CONTROLLING OFFICE NAME AND ADDRESS US Army Electronics Research and Development Command Adelphi, MD 20783		10. PROGRAM ELEMENT, PROJECT, TASK AREA & WORK UNIT NUMBERS DA Task No. 62111A-1L162111AH-71-DO
14. MONITORING AGENCY NAME & ADDRESS (if different from Controlling Office) 14 END COM/PE - TR-1121		12. REPORT DATE Feb 1980
		13. NUMBER OF PAGES 41
		15. SECURITY CLASS. (of this report) UNCLASSIFIED
		15a. DECLASSIFICATION/DOWNGRADING SCHEDULE
16. DISTRIBUTION STATEMENT (of this Report) Approved for public release; distribution unlimited. 6 11162111AH 11		
17. DISTRIBUTION STATEMENT (of the abstract entered in Block 20, if different from Report)		
18. SUPPLEMENTARY NOTES *Physical Science Laboratory New Mexico State University University Park, New Mexico 88003		
19. KEY WORDS (Continue on reverse side if necessary and identify by block number) Remote wind sensor Airborne laser Doppler velocimeter Helicopter wind fields		
20. ABSTRACT (Continue on reverse side if necessary and identify by block number) A flight test program has been completed in which the Helicopter Remote Wind Sensor was mounted on a UH-1 testbed aircraft. Wind measurements were made and recorded under a variety of flight hover conditions. Data from the flight test program are presented as wind profiles as a function of range, and data reduction and analysis approaches are discussed. The point-pair method was applied for comparison to theoretical and wind tunnel results. The data are applied to a baseline ballistics study sufficient to estimate the quantity of data needed for free-flight aerial armaments.		

CONTENTS

	<u>Page</u>
LIST OF FIGURES	4
LIST OF TABLES	5
INTRODUCTION	7
DATA REDUCTION AND ANALYSIS	7
General	7
Data Format	8
Principle of Operation and Conversion of Data	8
Data Analysis	10
BALLISTICS	11
CONCLUDING REMARKS	13
FIGURES	14
TABLES	24
REFERENCES	31
APPENDIX A	
Circular Scan Wind Reduction	32
APPENDIX B	
2.75-Inch FFAR Test Simulations	36

Accession For	
NTIS GNA&I	<input checked="checked" type="checkbox"/>
DDC TAB	<input type="checkbox"/>
Unannounced	<input type="checkbox"/>
Justification	
By _____	
Distribution/ _____	
Security Codes _____	
Dist	Avail and/or special
A	

LIST OF FIGURES

<u>Figure</u>		<u>Page</u>
1	Artist's concept of helicopter remote wind sensor (HRWS)	14
2	Helicopter remote wind sensor geometry; side view at level hover	15
3	Helicopter remote wind sensor; top view	16
4	Range versus digitized counts	17
5	Downwash profile: Wind tunnel (Landgrebe and Bennett)	18
6	Downwash profile: 3-foot hover	18
7	Downwash profile: 20-foot hover	19
8	Downwash profile: 50-foot hover	19
9	Downwash profile: 100-foot hover	20
10	Rectified biased sine function	21
11	Indicator function	21
12	Pitch-up due to downwash. Ripple of five 2.75-inch rockets from YAH-64	22
13	2.75-inch representative wind weighting functions	23
14	2.75-inch FFAR profile response functions	23

LIST OF TABLES

<u>Table</u>		<u>Page</u>
1	Operation Hiwind Test Schedule	24
2	Analog Tape Channel Assignments	25
3	Operation Hiwind Helicopter Tests Telemetry Computer Format	26
4	Range Calibration Volts, Counts, Range	27
5	Binary to Wind Velocity Conversion	28
6	Typical Profile Response Functions for Various Hover Heights and Wind Tunnel Results	29
7	Typical Downwash Profiles	30

INTRODUCTION

The purpose of the Helicopter Remote Wind Sensor (HRWS) (figure 1, artist's concept) is to provide measured wind data, including the downwash flow field, for ballistic corrections, by a fire control system for AH-1 or AAH aircraft. A test program has been completed in which the HRWS was mounted on a UH-1 testbed aircraft, and actual wind measurements were made and recorded in a variety of flight environments. Data were reduced and analyzed to determine the accuracy of measurement, quality of deduced wind profiles, and estimates of the amount (sample size) of data necessary for in-flight ballistic corrections. Simulation techniques have been applied to obtain wind weighting functions and total wind effects for a 2.75-in. folding fin aerial rocket (FFAR) to estimate the quantity and duration of measurements required of the HRWS for effective improvement in the accuracy of delivery of this particular free-flight armament.

The HRWS, system fabricated by Raytheon Company for the Atmospheric Sciences Laboratory, US Army Electronics Research and Development Command, is described in another report.¹

The HRWS test scheme (table 1) was devised to provide proof of the ability of the HRWS to perform in the helicopter flight environment and to measure winds in unprobed conditions, thereby building a data base for current and future studies of real helicopter flow-fields.

The test schedule consisted of two major parts:

1. Flights and data acquisition over level terrain, and
2. Flights and data acquisition over rough terrain, simulating tactical free-flight weapon firings.

DATA REDUCTION AND ANALYSIS*

General

The acquisition system consisted of a pair of Ampex analog tape units, one mounted in the helicopter and the other integrated into an analog-to-digital computer system. Field tapes of the flight tests were "played back" on this system, and the resulting raw digital data were transferred in real time to disk storage in an IBM 370 computer. Data

¹D. H. Dickson and C. M. Sonnenschein, 1979, "Helicopter Remote Wind Sensor System Description," R&D Tech Report ASL-TR-0040, US Army Atmospheric Sciences Laboratory, White Sands Missile Range, NM

*The Physical Science Laboratory of New Mexico State University, under contract DAAD07-76-C-0007, Task AP018, reduced and analyzed the data for this program.

are converted, stored, and displayed by a set of programs written to process HRWS data. Selected subsets of the data have been transferred to other computers for remote transmission and for analysis of various features observed in the data; approximately 46 megabytes of digitized data are stored in the system. These data and the converted data will be preserved on magnetic tape for future use.

Data Format

Eight channels of the analog tape were used to record the equivalent of seven bits of discrete data output by the HRWS final processor plus a data validity bit. In addition, four other channels were used to record the helicopter voice communication channel and the output of the HRWS zero marker, range, and voltage controlled oscillator (VCO) voltage level (table 2). Voice cues were used to begin and end digitized data sets associated with the various tests. Each data set is labelled by a unique identification number.

A transcript of the voice channel of each field tape provides requisite information about the particular test being performed, as well as wind reports and observations made by the flight and test personnel aboard. Digitized data have been packed into pairs of 16-bit words, each pair identified by appropriate frame marker bits. The peculiar structure of the pair is due to use of the existing digitizing system (table 3).

Principle of Operation and Conversion of Data

The HRWS essentially measures the component of relative velocity of the air at a point along the current line-of-sight which moves in a conical scan mode. The measurement is obtained via application of the Doppler principle.¹ HRWS discrete output directly represents the Doppler shift, while the VCO data represent an analog form of the shift. Range, the line-of-sight distance to the point of measurement, is a function of potentiometer voltage from the HRWS range scanner.

In the nominal mode of operation, the HRWS runs with both conical scan and range scan operating so that the point of measurement moves in a spiral pattern in the surface of the cone (figures 2 and 3). Thus, the time sequence of data can be represented as a scalar function of conical scan angle and range.

A clocking mechanism and a reference point (the "0-degree" marker) cause the HRWS to produce 128 well-defined sample points in each conical scan so that the data are fully discretized and each sample point has associated with it an angle and a range value. The conical scan rate is usually

¹D. H. Dickson and C. M. Sonnenschein, 1979, "Helicopter Remote Wind Sensor System Description," R&D Tech Report ASL-TR-0040, US Army Atmospheric Sciences Laboratory, White Sands Missile Range, NM

set much higher than the range scan rate so that, in a typical flight test, the average change of range in a conical scan is approximately 2 feet. The authors take advantage of this condition in analysis of data by assuming a fixed range for given conical scan, thus simplifying deduction of wind components.

The basic digitized data are: (1) discrete output of frequency shift, (2) digitized VCO voltage, and (3) digitized voltage representing range; all taken at conical scan angles whose values are known with respect to a reference. Note: With the HRWS mounted on the helicopter, the cone axis is parallel to the centerline, the angle "0 degrees" is in the vertical, and the scan angle is plus counterclockwise, looking forward. HRWS contains a self-calibrating feature with respect to the discrete frequency shift output; thus, the conversion to windspeed (along the line-of-sight) is of the form

$$|V_d| = K |\Delta f| ,$$

where

$|V_d|$ is the absolute Doppler "velocity,"

$|\Delta f|$ is the Doppler frequency, and

K is the reference frequency wavelength.

K is used here because the discrete output least significant bit has a given frequency value which is lumped together with the wavelength, λ .

Conversion of VCO was not so straightforward. The flight test series was performed by a discriminator calibration which determined VCO voltage versus frequency. The flight test tapes generally contained (at the beginning of a set of tests as a requirement) a voltage calibration of the VCO channel plus a 2 MHz tone burst. So, in principle, a calibration function was produced through which VCO data were converted to frequency shift and then to Doppler speed.

Subsequent discriminator calibrations have shown that shifts due to use or "burn-in" occurred throughout the test series. No autocalibration procedure has been applied in the conversion of VCO voltage to Doppler speed; hence, the VCO speed deduced can be different from the discrete equivalent by ± 1.5 m/s.

Conversion of range voltage to range in distance units (figures 4 and 5; table 4) has been most difficult because of the nature of the HRWS optical system. In this case, the lens equation was to have been applied, along with image distance as a function of voltage. The resulting function is of hyperbolic form such that at small voltage (long range),

uncertainties due to sampling and actual range value measurement lead to large variations in deduced range and also to large biases for large values of deduced range.

Generally, the digitized range voltage on a scale of 0 to 255 is used in most presentations of data, rather than converted range in distance units. Where display or other results are shown graphically, an alternative scale is shown in parallel with the data.

Data Analysis

Note that HRWS initial design was aimed at measurements out to approximately 100 ft from the sensor origin (cone apex). Further, the sensor is a descendent of other conical scanning devices whose domain of measure was considerably less turbulent and less subject to linear shear than that in a helicopter's vicinity. Wind tunnel and other measurement studies demonstrate the complexity of the helicopter flow field.²

To maximize the spacial (geometric) resolution of wind, the HRWS cone angle was set at the largest value attainable under the test requirements. By contrast, the cone diameter at a given range in the order of helicopter rotor radius is approximately 1/3 that radius. Further, the cone angle is such that the laser line-of-sight passes very close to the testbed aircraft's canopy and fuselage.

Two simplified approaches have been applied in the data analysis: (1) circular scan methods, and (2) point-pair methods. Considering the latter, which is the simplest: any pair of points separated by a sufficient angle can be used to deduce the wind components transverse to, as well as parallel to, the axis halfway between them. A table has been devised for the extreme case in this approach: (Note: extreme means the widest separation of points, i.e., points 180 degrees apart in conical scan angle.)

The point-pair method has been applied to derive downwash profiles as running functions of range over a short sequence of range scans for comparison to theoretical and wind tunnel results.

Circular scan methods are based on an assumption that, in the data, the range change over a conical scan can be ignored so that a single conical scan is made equivalent to a circular scan at a fixed range.

A second simplifying and realistic assumption is applied: Over a single circular scan the wind is constant. The result of combination of these

²A. J. Landgrebe and J. C. Bennett, Jr., 1977, "Investigation of the Airflow of a Hovering Model Helicopter at Rocket Trajectory and Wind Sensor Locations," United Technologies Research Center, Report R77-912573-15

assumptions is that the HRWS measurements over a given circular scan at fixed range in a constant wind can be represented as rectified sinusoidal functions (table 5). Rectification is the result of the fact that the HRWS output is unsigned. A method for computing wind from circular scan data has been derived and tested on selected flight test results (table 6; figures 5, 6, 7, 8, and 9). The derivation and its equations are contained in appendix A.

Essentially, the equations show a method for calculating the equivalent of the first three terms of a Fourier series on the data. The unique aspect of this analytical-mathematical approach is that the rectified data (absolute values) (figure 10) are accounted for by decomposition of the integral forms into signed segments.

These signed segments can also be treated as though an indicator function had acted upon an originally signed signal (figure 11).

An application of the least-squares principle is then made to determine optimum values of ϕ_s and ϕ_e , i.e., ϕ_s and ϕ_e such that S , the weighted sum of squared residuals, is minimized. A weighting function is generally required so that ground (surface) effects and invalid points can be masked out of flow field data.

BALLISTICS

An objective of the HRWS tests was to provide a baseline ballistics study sufficient to estimate ranging requirements and quantity of data for a given free-flight armament, in this case, the 2.75-in. FFAR.

A rocket is most sensitive to the effects of wind in its burn phase (figure 12). The duration of the 2.75-in. FFAR burn phase is approximately 1.6 s. The burning trajectory of the FFAR is most sensitive to the helicopter flow field³ (figure 12 of ref 3).

Tables necessary to simulate trajectories of the 2.75-in. rocket have been obtained from various sources and are contained in appendix B. Sensitivity functions sufficient to determine what might be required of an in-flight wind measurement system and of a fire control system have been derived from simulation. Sensitivity to wind is expressed by a wind weighting function, which is a statement of how much a free-flight armament's miss due to wind depends on a unit wind acting over a given portion of its trajectory, and is defined by

³S. Wasserman and R. Yellir, "Preliminary Analysis of the Effect of Calculated Downwash Distributions on the 2.75-Inch Rocket," presented at technical conference on "The Effects of Helicopter Downwash on Free Projectiles," US Army Aviation Systems Command, St. Louis, Missouri, 12-14 August 1975

$$f(l) = \frac{x_l - x_0}{x_L - x_0},$$

where l is the distance a unit wind acts over the trajectory, starting at launch; L is the maximum distance the wind is allowed to act; and x is the coordinate of interest, usually range to impact or crossrange displacement.

The wind weighting function implies, for a given profile, what extent with respect to the variable of integration a given percentage of a total wind field should be represented to account for a fixed percentage of that profile's effect. More than one variable is involved in this tradeoff, and the wind profile shape is important. The weighting functions (figure 13) show that approximately 70 percent of the rocket response to a unit wind occurs by the time it has travelled only 30 ft from launch. However, the wind profile is such that the largest wind velocities generally occur within that same distance interval. A second function, called here the profile response function (table 6; figure 14), is derived from the weighting functions and a set of profiles. This second function is defined by

$$P(l) = \frac{\int_0^l w(\tau) f'(\tau) d\tau}{\int_0^L w(\tau) f'(\tau) d\tau},$$

where w is the wind profile. The response function shows how much the profile affects the miss due to wind and thus implies the relative importance of wind measurement as a function of distance. A set of downwash profiles was taken from the flight test data to evaluate the response function (table 7).

The results illustrate the value of measurement out to approximately 300 ft. Measurements at longer ranges are valuable. Instrumentation and accuracy tradeoffs will be pursued as more definitive error budgets become available.

In any case, the measurement of wind to 300 ft gives 96 percent or more of the total wind response.

The curves also indicate that the differences between profiles at various hover heights and various flight conditions are important and require measurement to improve accuracy of delivery.

CONCLUDING REMARKS

Measurement of wind by the Helicopter Remote Wind Sensor in hovering flight and in simulated firings over nap of the earth terrain has resulted in a large data base for helicopter flow field and ballistic analyses. Methods for reducing wind in component form have been developed and applied to measured data. Selected downwash profiles from the data and wind sensitivity functions from simulated 2.75-in. rocket trajectories have been used to estimate the relative importance of measurement as a function of distance for the particular armament. Future analysis using rocket error budgets and improved wind reduction methods is planned for a potential fire control system.

Data were successfully obtained, reduced, and analyzed for all test flights. The aircraft hover cases generally agree with the wind tunnel measurements. Variation in windspeed magnitudes are readily attributed to physical differences in aircraft and the in- or out-of-ground effect flight conditions; however, the general curve slope remains basically the same for all profiles over semiflat terrain.

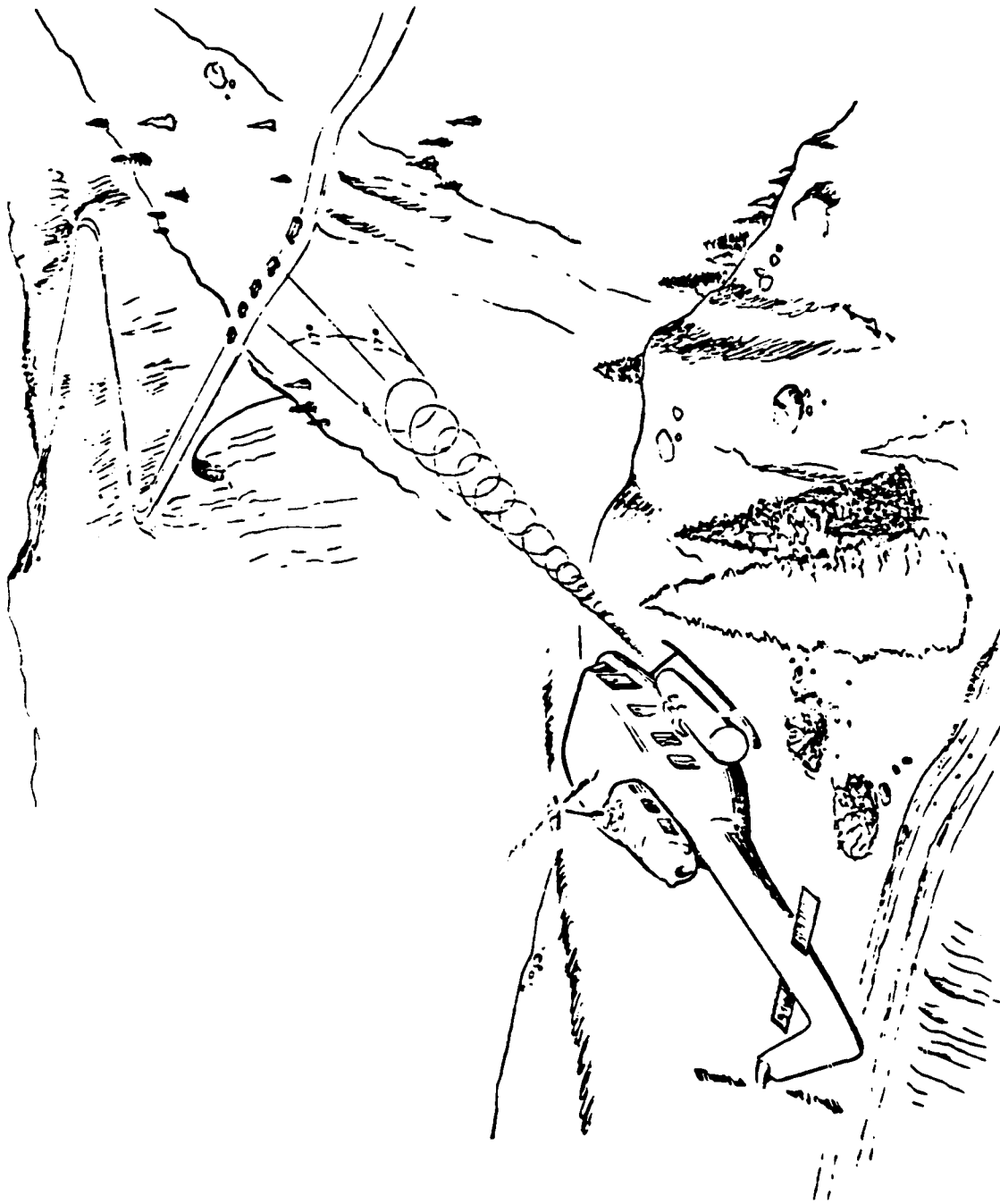


Figure 1. Artist's concept of helicopter remote wind sensor (HRWS).

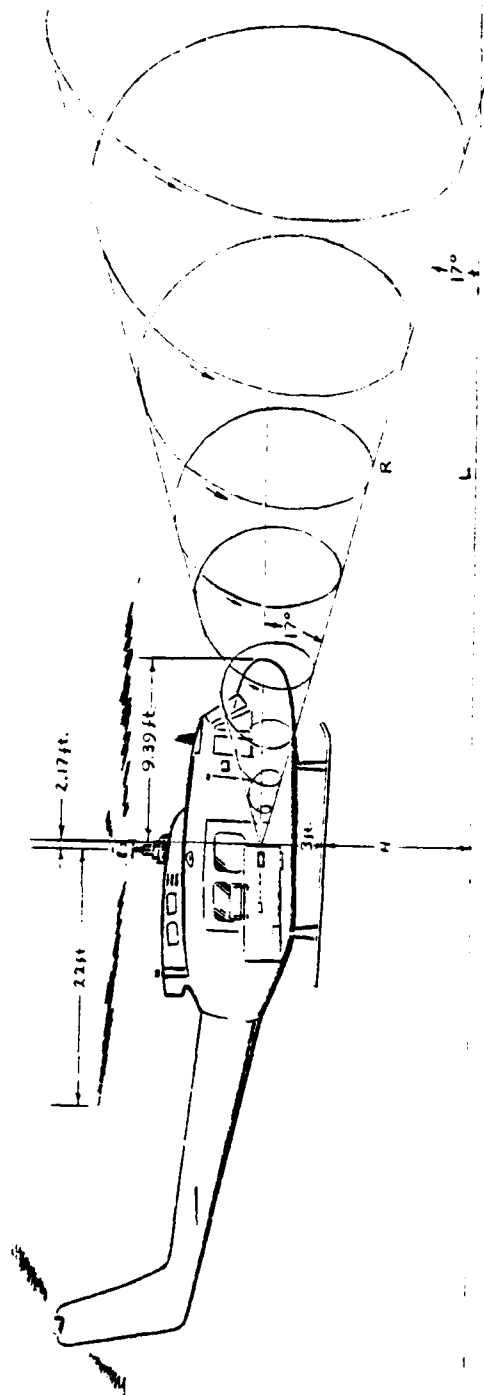


Figure 2. Helicopter remote wind sensor geometry; side view at level hover.

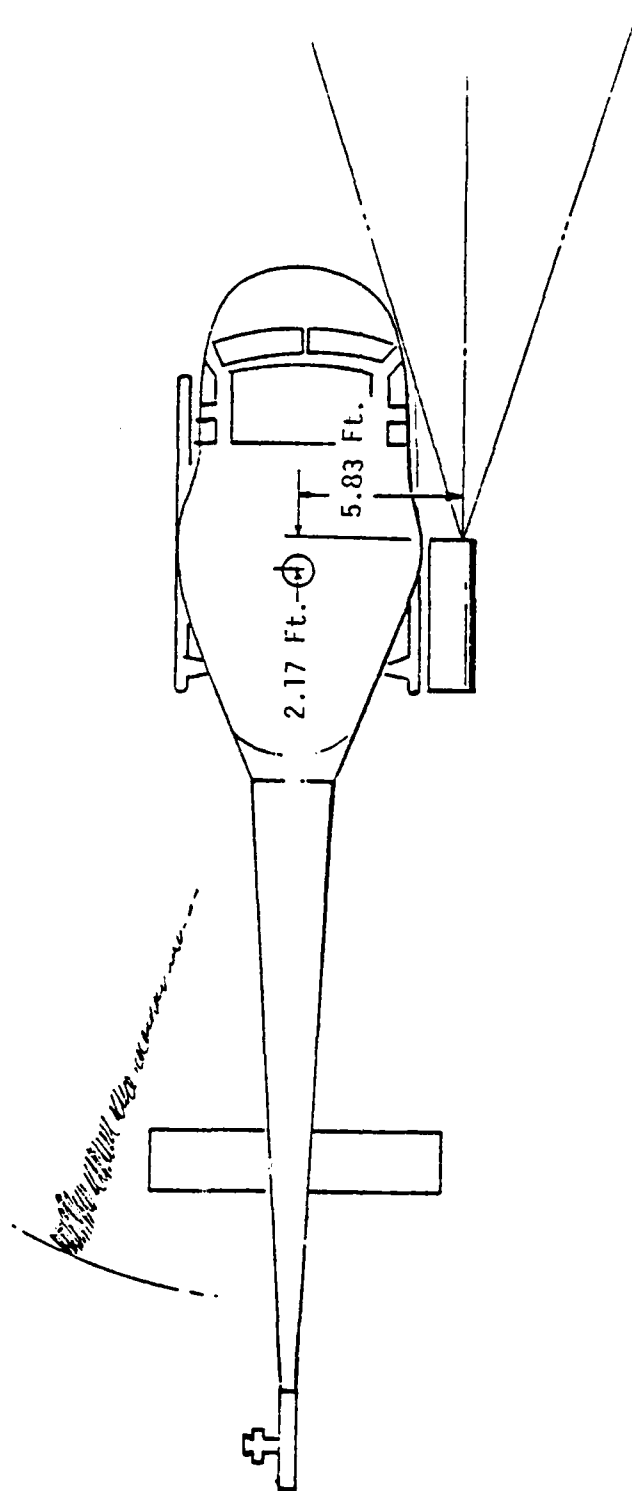


Figure 3. Helicopter remote wind sensor; top view.

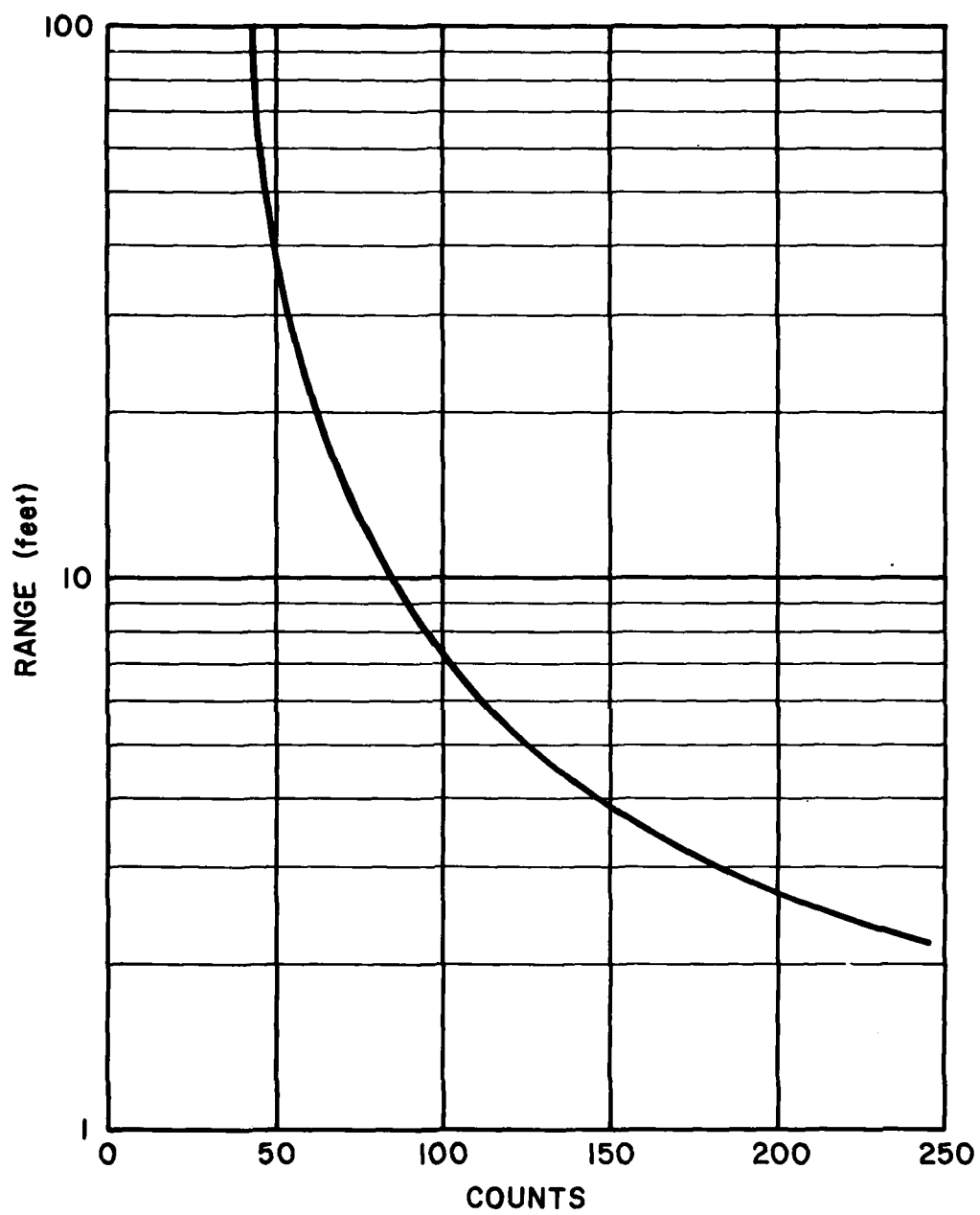


Figure 4. Range versus digitized counts.

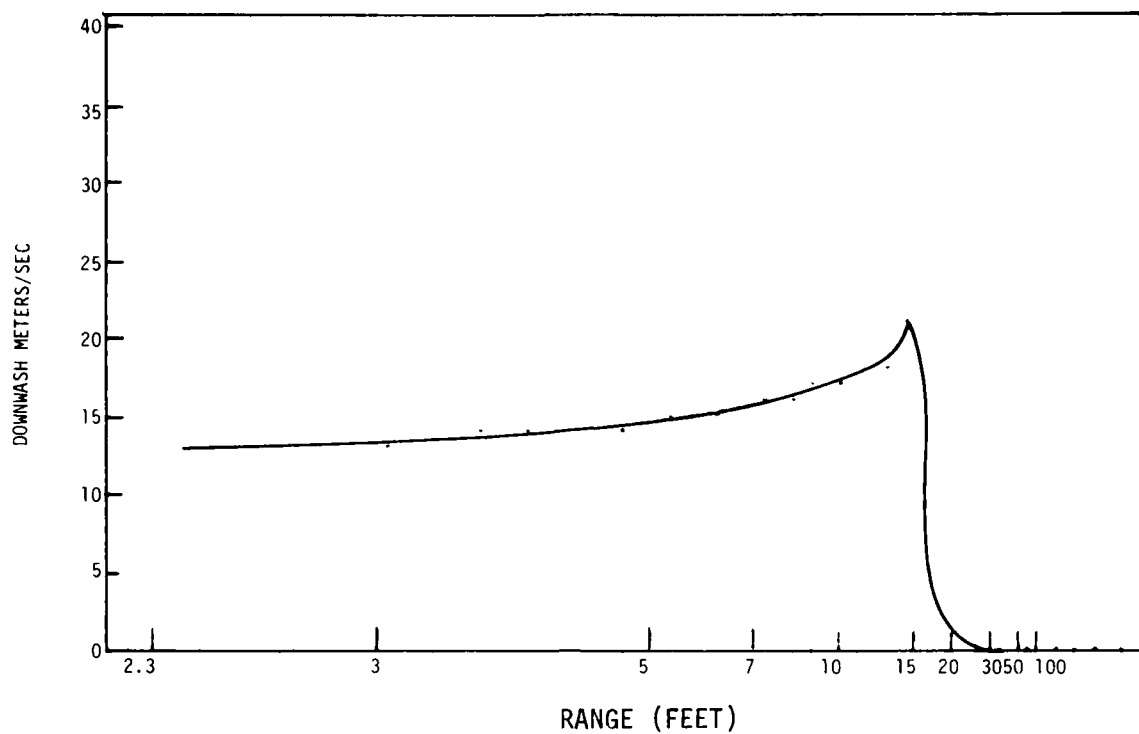


Figure 5. Downwash profile: Wind tunnel (Landgrebe and Bennett).

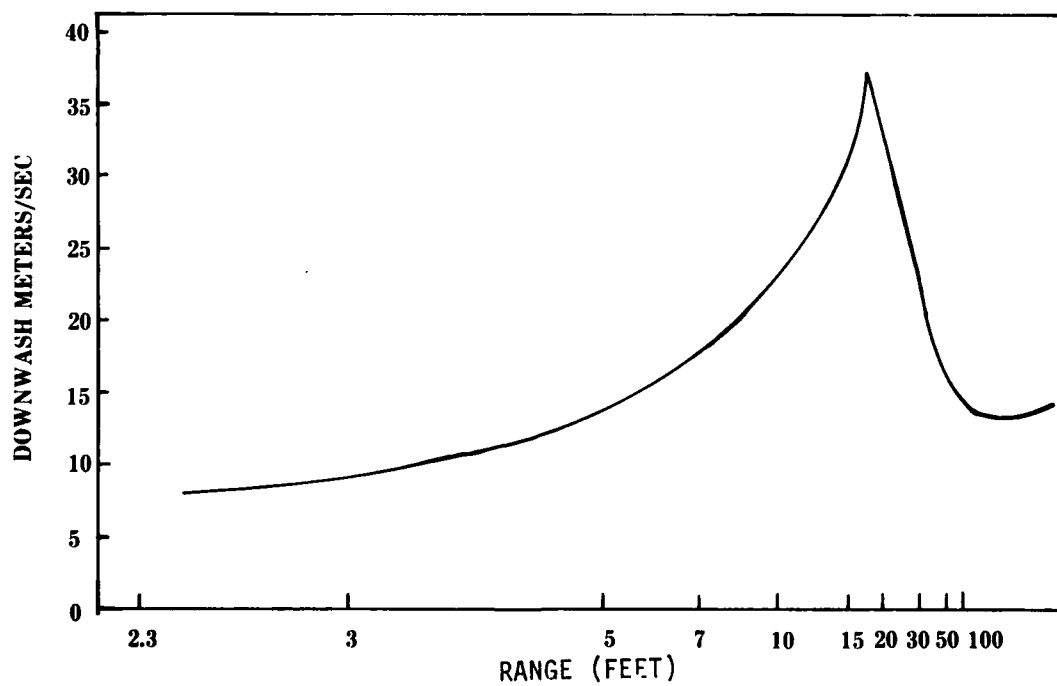


Figure 6. Downwash profile: 3-foot hover.

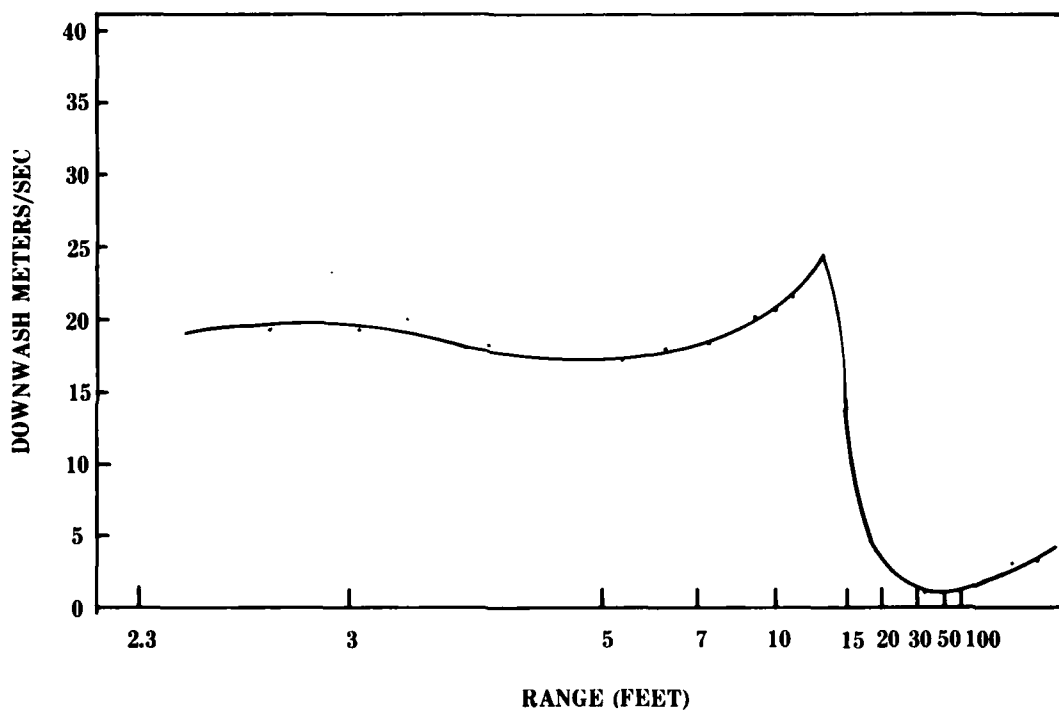


Figure 7. Downwash profile: 20-foot hover.

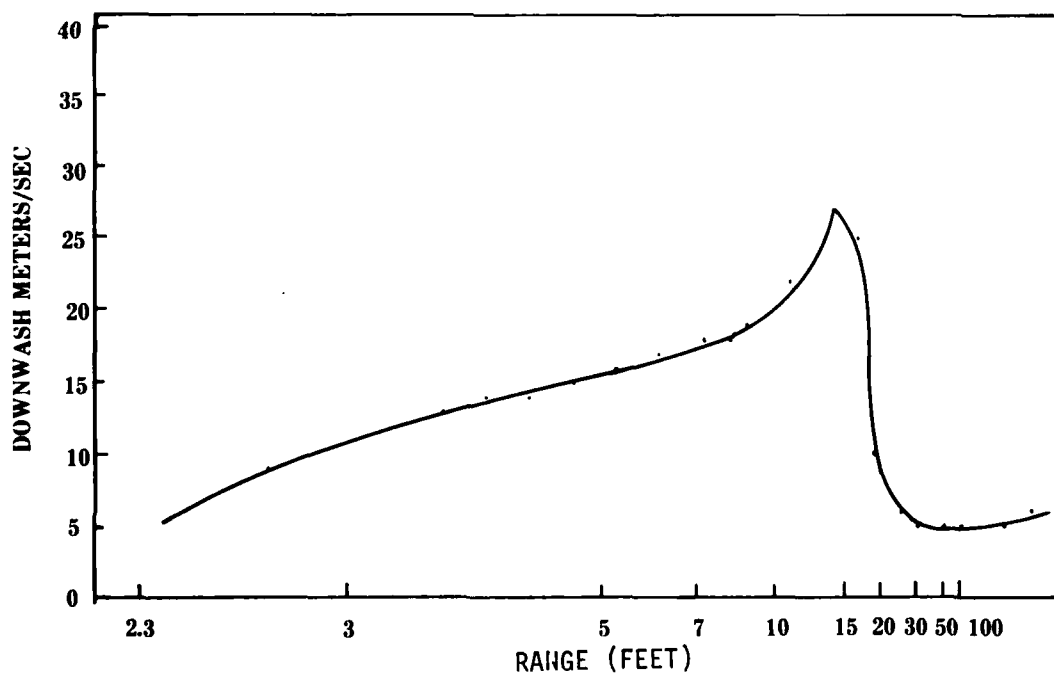


Figure 8. Downwash profile: 50-foot hover.

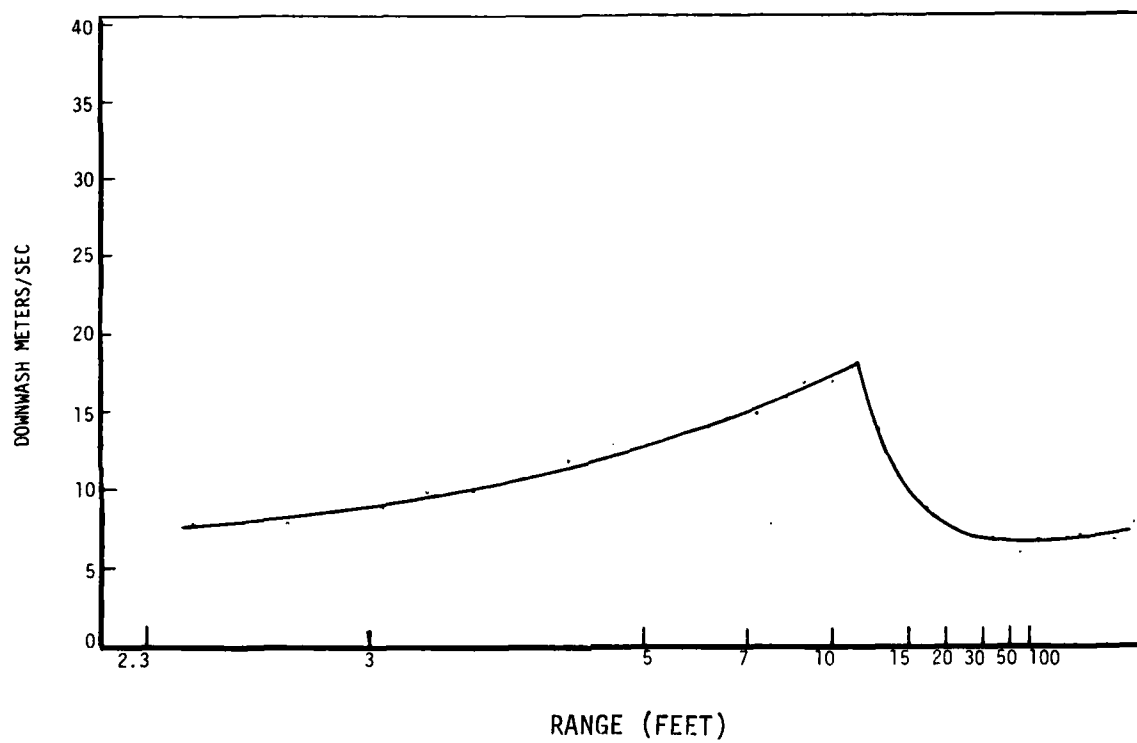


Figure 9. Downwash profile: 100-foot hover.

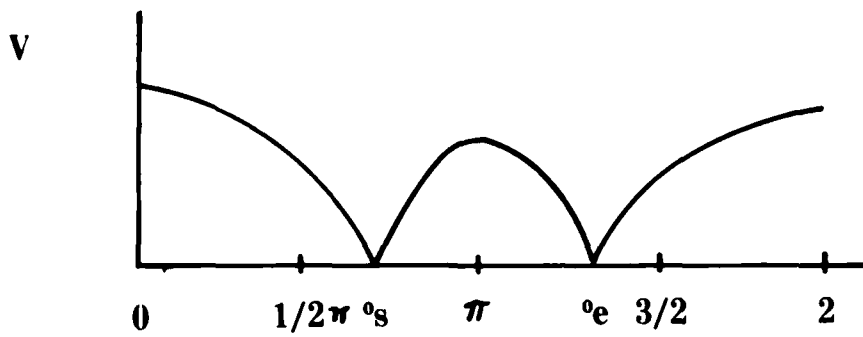


Figure 10. Rectified biased sine function.

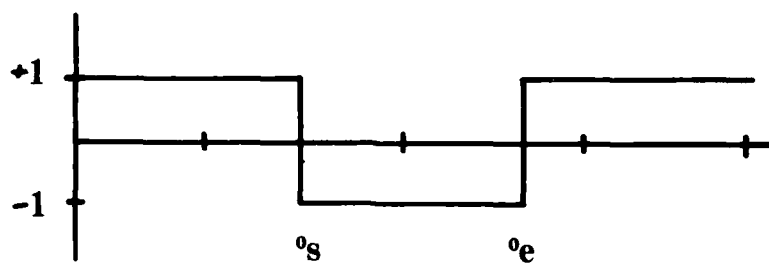


Figure 11. Indicator function.



Figure 12. Pitch-up due to downwash. Ripple of five 2.75-in. rockets from YAH-64.

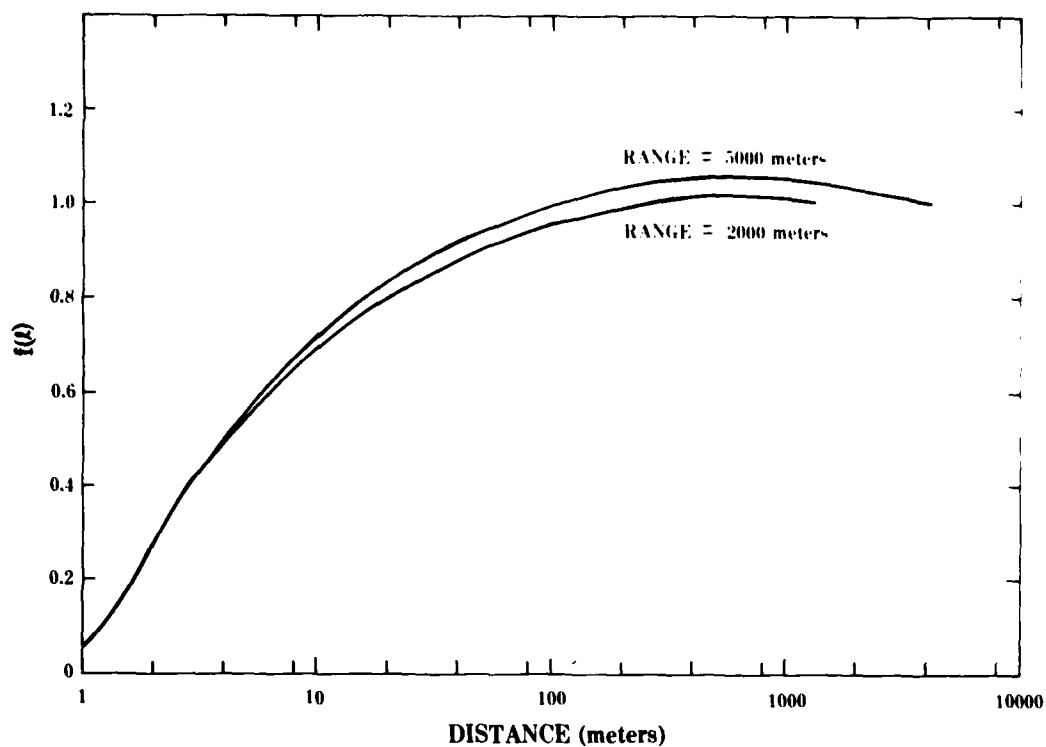


Figure 13. 2.75-inch representative wind weighting functions.

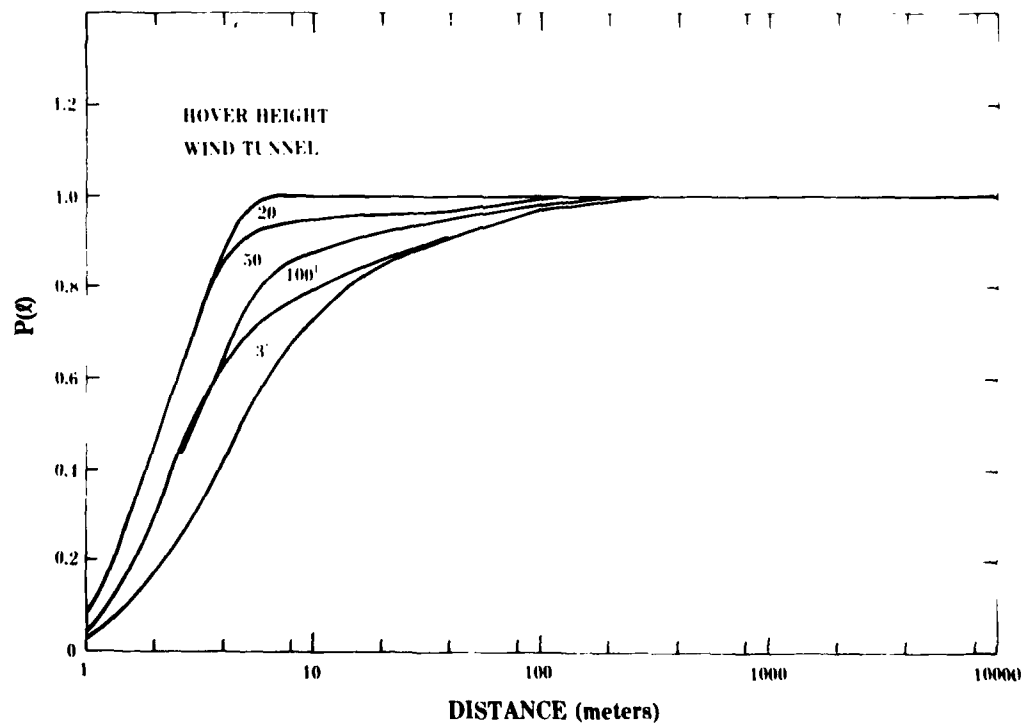


Figure 14. 2.75-inch FFAR profile response functions.

TABLE 1. OPERATION HIWIND TEST SCHEDULE

<u>DATE</u> <u>(Mar 78)</u>	<u>Flight</u>	<u>Reel</u>	<u>Description</u>
15	1	1	Preliminary hover checks, 500-ft hover
		2	Preliminary hover checks, 10- to 20-ft hover
16	2	1	3-ft hover
17	3	1	50-ft hover
		2	50- to 100-ft transition, 100-ft hover
17	4	1	Popups: 3 to 35 ft, 24-ft hover
			3 to 50 ft, 50-ft hover
			3 to 100-ft, 100-ft hover
17	5	1	Nap-of-the-earth (NOE) simulated popup
			20-mm cannon, 40-mm grenade launcher, and 2.75 in. FFAR
21	6	1	NOE simulated popup and fire 2.75-in. FFAR from behind various shallow, steep, and rough hills.
		2	Same as reel 1, including lateral unmasking and unmasking from a saddle.

TABLE 2. ANALOG TAPE CHANNEL ASSIGNMENTS

<u>Channel</u>	<u>Data</u>
1	Data clock
2	Validity
3	F3
4	F4
5	F5
6	F6
7	F7
8	F8
9	F9
10	0° marker
11	Range
12	Voice
13	VCO
14	Control track

7 bits
discrete
data

TABLE 3. OPERATION HIRIND HELICOPTER TESTS
TELEMETRY COMPUTER FORMAT

From the FM/FM telemetry computer format, the output was modified for digitizing the HRKS data to give a data frame as follows:

Word No.	Bit Positions															
	0	1	2	3	4	5	6	7	8	9	10	11	12	13	14	15
	MSB							LSB								
0	← RANGE →															
	2^7	2^6	2^5	2^4	2^3	2^2	2^1	2^0	F_9	F_8	F_7	F_6	0	"0"	1	1
1	← VCO →															
									F_5	F_4	F_3	V	0	"0"	0	0

Timing was removed and digital data placed in timing positions of words 0 and 1.

The analog range and VCO voltages from the tape were amplified, and range was level shifted for a \pm volt input to the A/D converter.

TABLE 4. RANGE CALIBRATION VOLTS, COUNTS, RANGE

<u>Volts</u>	<u>Counts</u>	<u>Range (ft)</u>
0.132	43.0	100
0.136	43.8	75
0.150	47.0	50
0.196	57.1	25
0.253	70.0	12.5
0.317	84.0	10
0.379	97.7	7.5
0.505	124.3	5
0.600	145.6	4
0.766	180.7	3
0.910	211.0	2.5
1.000	229.6	2.3

TABLE 5. BINARY TO WIND VELOCITY CONVERSION

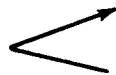


Channel	Word	Bit	Frequency (Hz)			
				Velocity Along Beam	Longitudinal Velocity	Transverse Velocity
F-9	0	8	6.4×10^6	34 m/s 66 kn	35 m/s 69 kn	116 m/s 226 kn
F-8	0	9	3.2×10^6	17 m/s 33 kn	18 m/s 34 kn	58 m/s 113 kn
F-7	0	10	1.6×10^6	8.5 m/s 16 kn	8.9 m/s 17 kn	29 m/s 56 kn
F-6	0	11	8.0×10^5	4.2 m/s 8.2 kn	4.4 m/s 8.6 kn	14 m/s 28 kn
F-5	1	8	4.0×10^5	2.1 m/s 4.1 kn	2.2 m/s 4.3 kn	7.3 m/s 14 kn
F-4	1	9	2.0×10^5	1.1 m/s 2.1 kn	1.1 m/s 2.2 kn	3.6 m/s 7.0 kn
F-3	1	10	1.0×10^5	0.53 m/s 1.0 kn	0.55 m/s 1.1 kn	1.8 m/s 3.5 kn
F-2	-	-	5.0×10^4	0.26 m/s 0.51 kn	0.28 m/s 0.54 kn	0.91 m/s 1.8 kn
F-1	-	-	2.5×10^4	0.13 m/s 0.26 kn	0.14 m/s 0.27 kn	0.45 m/s 0.88 kn
F-0	-	-	1.25×10^4	0.066 m/s 0.13 kn	0.069 m/s 0.13 kn	0.23 m/s 0.44 kn

TABLE 6. TYPICAL PROFILE RESPONSE FUNCTIONS FOR VARIOUS HOVER HEIGHTS
AND WIND TUNNEL RESULTS

Distance (m)	Wind Tunnel (m)	3-ft Hover (m)	20-ft Hover (m)	50-ft Hover (m)	100-ft Hover (m)
0.760	0.000	0.000	0.000	0.000	0.000
0.834	0.025	0.007	0.028	0.010	0.012
0.935	0.059	0.016	0.067	0.027	0.030
1.041	0.094	0.027	0.108	0.049	0.051
1.146	0.132	0.040	0.149	0.072	0.074
1.251	0.170	0.053	0.189	0.097	0.099
1.356	0.209	0.067	0.228	0.124	0.125
1.461	0.249	0.083	0.266	0.152	0.153
1.635	0.313	0.110	0.325	0.198	0.200
1.912	0.416	0.158	0.421	0.275	0.278
2.235	0.510	0.205	0.506	0.344	0.350
2.489	0.576	0.239	0.566	0.394	0.402
2.743	0.643	0.277	0.628	0.446	0.456
2.997	0.712	0.317	0.693	0.500	0.513
3.454	0.781	0.360	0.757	0.556	0.570
3.962	0.859	0.411	0.835	0.623	0.627
4.470	0.918	0.451	0.879	0.675	0.657
5.334	0.980	0.528	0.916	0.763	0.697
6.477	0.993	0.611	0.932	0.826	0.734
8.382	0.998	0.690	0.941	0.859	0.771
12.192	1.000	0.767	0.949	0.886	0.813
21.336	1.000	0.852	0.957	0.919	0.868
36.576	1.000	0.900	0.964	0.940	0.905
51.816	1.000	0.929	0.971	0.955	0.930
67.056	1.000	0.940	0.974	0.961	0.940
82.296	1.000	0.951	0.978	0.968	0.951
97.536	1.000	0.963	0.983	0.975	0.962
10000.000	1.000	1.000	1.000	1.000	1.000

TABLE 7. TYPICAL DOWNWASH PROFILES

Range (Counts)	Wind Tunnel (m/s)	3-ft Hover (m/s)	20-ft Hover (m/s)	50-ft Hover (m/s)	100-ft Hover (m/s)
20	0.0	13.5	3.5	6.0	7.5
25	0.0	13.5	3.0	5.5	7.0
30	0.0	13.0	2.5	5.0	6.5
35	0.0	13.0	2.0	4.5	6.5
40	0.0	14.0	1.5	4.5	6.5
45	0.0	16.0	1.0	4.5	6.0
50	0.0	19.5	1.0	4.5	6.5
55	0.5	25.5	1.5	6.0	7.0
60	1.0	31.0	2.0	9.5	7.5
65	4.0	37.0	5.5	25.0	9.0
70	21.0	32.0	13.5	27.0	10.5
75	18.0	27.0	23.5	28.5	13.5
80	17.5	25.0	21.0	21.5	18.0
85	17.0	22.5	20.0	20.0	17.0
90	16.5	21.0	19.5	19.0	16.5
95	16.0	19.5	18.5	18.0	15.5
100	16.0	18.0	18.0	17.5	15.0
110	15.0	16.0	17.5	16.5	14.0
120	14.5	14.5	17.0	15.5	13.0
130	14.0	13.0	16.5	15.0	12.5
140	14.0	11.5	17.0	14.0	11.5
150	13.5	10.5	17.5	13.5	11.0
160	13.5	10.0	18.0	12.5	10.0
170	13.0	9.5	18.5	12.0	9.5
180	13.0	8.5	19.0	11.0	9.0
200	13.0	8.0	19.0	9.0	8.0
220	13.0	7.5	18.5	6.0	7.5

REFERENCES

1. Dickson, D. H., and C. M. Sonnenschein, 1979, "Helicopter Remote Wind Sensor System Description," R&D Tech Report ASL-TR-0040, US Army Atmospheric Sciences Laboratory, White Sands Missile Range, NM.
2. Landgrebe, A. J., and J. C. Bennett, Jr., 1977, "Investigation of the Airflow of a Hovering Model Helicopter at Rocket Trajectory and Wind Sensor Locations," United Technologies Research Center, Report R77-912573-15.
3. Wasserman S., and R. Yellir, "Preliminary Analysis of the Effect of Calculated Downwash Distributions on the 2.75-Inch Rocket," presented at technical conference on "The Effects of Helicopter Downwash on Free Projectiles," US Army Aviation Systems Command, St. Louis, Missouri, 12-14 August 1975.

APPENDIX A

CIRCULAR SCAN WIND REDUCTION

Let

- ε be the cone half-angle
- ϕ be the scan angle
- $m(\phi)$ be the measured doppler magnitude
- $s(\phi)$ be the indicator function
- $w(\phi)$ be the weighting function
- w_x be the wind along the cone axis
- w_y be the cross-wind
- w_z be the "vertical" wind

Then define $\eta(\phi)$ as the residual function:

$$\eta(\phi) = w(\phi) [s(\phi) m(\phi) - (w_x \cos \varepsilon + w_y \sin \varepsilon \sin \phi + w_z \sin \varepsilon \cos \phi)]$$

The data are obtained as 128 discrete points around a circular scan at angles

$$\phi_i = \frac{2\pi(i-1)}{n}, \quad i = 1, 2, \dots, n = 128.$$

Now define S as the normalized sum of the squared residuals:

$$S = \frac{1}{n} \sum_{i=1}^n w_i^2(\phi_i) [S(\phi_i) m(\phi_i) - (w_x \cos \varepsilon + w_y \sin \varepsilon \sin \phi_i + w_z \sin \varepsilon \cos \phi_i)]^2.$$

Thus, expanding,

$$\begin{aligned} S = & \frac{1}{n} \sum_{i=1}^n w_i^2 m_i^2 - \frac{2}{n} \sum_{i=1}^{n_s-1} w_i m_i (w_x \cos \varepsilon + w_y \sin \varepsilon \sin \phi_i + w_z \sin \varepsilon \cos \phi_i) \\ & + \frac{2}{n} \sum_{i=n_s}^{n_e-1} w_i m_i (w_x \cos \varepsilon + w_y \sin \varepsilon \sin \phi_i + w_z \sin \varepsilon \cos \phi_i) \\ & - \frac{2}{n} \sum_{i=n_e}^n w_i m_i (w_x \cos \varepsilon + w_y \sin \varepsilon \sin \phi_i + w_z \sin \varepsilon \cos \phi_i) \\ & + \frac{1}{n} \sum_{i=1}^n w_i^2 (w_x \cos \varepsilon + w_y \sin \varepsilon \sin \phi_i + w_z \sin \varepsilon \cos \phi_i)^2. \end{aligned}$$

We seek to minimize S by appropriate choice of

$$w_x, w_y, w_z, n_s, \text{ and } n_e.$$

Taking partial derivatives with respect to the wind,

$$\begin{aligned} \frac{\partial S}{\partial w_x} = 0 = & -\frac{2\cos\epsilon}{n} \sum_{i=1}^{n_s-1} w_i^2 m_i + \frac{2\cos\epsilon}{n} \sum_{i=n_s}^{n_e-1} w_i^2 m_i - \frac{2\cos\epsilon}{n} \sum_{i=n_e}^n w_i^2 m_i \\ & + \frac{2\cos\epsilon}{n} \sum_{i=1}^n w_i^2 (w_x \cos \epsilon + w_y \sin \epsilon \sin \phi_i + w_z \sin \epsilon \cos \phi_i) \end{aligned}$$

$$\begin{aligned} \frac{\partial S}{\partial w_y} = 0 = & -\frac{2\sin\epsilon}{n} \sum_{i=1}^{n_s-1} w_i^2 m_i \sin \phi_i + \frac{2\sin\epsilon}{n} \sum_{i=n_s}^{n_e-1} w_i^2 m_i \sin \phi_i \\ & - \frac{2\sin\epsilon}{n} \sum_{i=n_e}^n w_i^2 m_i \sin \phi_i + \frac{2\sin\epsilon}{n} \sum_{i=1}^n w_i^2 (w_x \cos \epsilon + w_y \sin \epsilon \sin \phi_i \\ & + w_z \sin \epsilon \cos \phi_i) \sin \phi_i \end{aligned}$$

$$\begin{aligned} \frac{\partial S}{\partial w_z} = 0 = & -\frac{2\sin\epsilon}{n} \sum_{i=1}^{n_s-1} w_i^2 m_i \cos \phi_i + \frac{2\sin\epsilon}{n} \sum_{i=n_s}^{n_e-1} w_i^2 m_i \cos \phi_i \\ & - \frac{2\sin\epsilon}{n} \sum_{i=n_e}^n w_i^2 m_i \cos \phi_i + \frac{2\sin\epsilon}{n} \sum_{i=1}^n w_i^2 (w_x \cos \epsilon + w_y \sin \epsilon \sin \phi_i \\ & + w_z \sin \epsilon \cos \phi_i) \cos \phi_i \end{aligned}$$

Eliminating common constants and rearranging,

$$\begin{bmatrix} \sum_{i=1}^n w_i^2 & \sum_{i=1}^n w_i^2 \sin \phi_i & \sum_{i=1}^n w_i^2 \cos \phi_i \\ \sum_{i=1}^n w_i^2 \sin \phi_i & \sum_{i=1}^n w_i^2 \sin^2 \phi_i & \sum_{i=1}^n w_i^2 \sin \phi_i \cos \phi_i \\ \sum_{i=1}^n w_i^2 \cos \phi_i & \sum_{i=1}^n w_i^2 \sin \phi_i \cos \phi_i & \sum_{i=1}^n w_i^2 \cos^2 \phi_i \end{bmatrix} \begin{bmatrix} w_x \cos \epsilon \\ w_y \sin \epsilon \\ w_z \cos \epsilon \end{bmatrix} = \begin{bmatrix} I_1 \\ I_2 \\ I_3 \end{bmatrix},$$

where

$$I_1 = \sum_{i=1}^{n_s-1} w_i^2 m_i - \sum_{i=n_s}^{n_e-1} w_i^2 m_i + \sum_{i=n_e}^n w_i^2 m_i$$

$$I_2 = \sum_{i=1}^{n_s-1} w_i^2 m_i \sin \phi_i - \sum_{i=n_s}^{n_e-1} w_i^2 m_i \sin \phi_i + \sum_{i=n_e}^n w_i^2 m_i \sin \phi_i$$

$$I_3 = \sum_{i=1}^{n_s-1} w_i^2 m_i \cos \phi_i - \sum_{i=n_s}^{n_e-1} w_i^2 m_i \cos \phi_i + \sum_{i=n_e}^n w_i^2 m_i \cos \phi_i$$

We have also the side conditions

$$W_x \cos \varepsilon + W_y \sin \varepsilon \sin \phi_{n_s} + W_z \sin \varepsilon \cos \phi_{n_s} = 0$$

$$W_x \cos \varepsilon + W_y \sin \varepsilon \sin \phi_{n_e} + W_z \sin \varepsilon \cos \phi_{n_e} = 0$$

where the approximation is due to the discrete sampling of the scan data.
The side conditions do not hold if there is no rectification of the sinusoidal scan data.

Thus the system of equations to be solved is of the form:

$$[M] \begin{pmatrix} W_x \cos \varepsilon \\ W_y \sin \varepsilon \\ W_z \sin \varepsilon \end{pmatrix} = \begin{pmatrix} I_1 \\ I_2 \\ I_3 \end{pmatrix},$$

$$W_x \cos \varepsilon + W_y \sin \varepsilon \sin \phi_{n_s} + W_z \cos \phi_{n_s} = 0$$

$$W_x \cos \varepsilon + W_y \sin \varepsilon \sin \phi_{n_e} + W_z \cos \phi_{n_e} = 0$$

Given n_s, n_e as trial values,

$$\begin{pmatrix} w_x \cos \varepsilon \\ w_y \sin \varepsilon \\ w_z \sin \varepsilon \end{pmatrix} = [M^{-1}] \begin{pmatrix} I_1 \\ I_2 \\ I_3 \end{pmatrix} = \begin{pmatrix} V_1 \\ V_2 \\ V_3 \end{pmatrix},$$

we have to resolve

$$d_1 = V_1 + V_2 \sin \phi_{n_s} + V_3 \cos \phi_{n_s}$$

$$d_2 = V_1 + V_2 \sin \phi_{n_e} + V_3 \cos \phi_{n_e}.$$

Utilizing psuedo-derivatives, we define

$$\begin{pmatrix} \hat{d}_1 \\ \hat{d}_2 \end{pmatrix} \doteq [D] \begin{pmatrix} \Delta \phi_{n_s} \\ \Delta \phi_{n_e} \end{pmatrix} + \begin{pmatrix} d_1 \\ d_2 \end{pmatrix}$$

where

$$[D] \doteq \begin{bmatrix} \frac{\partial d_1}{\partial \phi_{n_s}} & \frac{\partial d_1}{\partial \phi_{n_e}} \\ \frac{\partial d_2}{\partial \phi_{n_s}} & \frac{\partial d_2}{\partial \phi_{n_e}} \end{bmatrix}.$$

Then, for $\hat{d}_1 = 0$ and $\hat{d}_2 = 0$

$$\begin{pmatrix} \Delta \phi_{n_s} \\ \Delta \phi_{n_e} \end{pmatrix} = -[D]^{-1} \begin{pmatrix} d_1 \\ d_2 \end{pmatrix}$$

is used to adjust the trial values

$$\begin{aligned} \phi_{n_s} &\leftarrow \Delta \phi_{n_s} + \phi_{n_s} \\ \phi_{n_e} &\leftarrow \Delta \phi_{n_e} + \phi_{n_e} \end{aligned}$$

and the process is repeated until

$$d_1 \doteq 0 \text{ and } d_2 \doteq 0.$$

APPENDIX B

2.75-INCH FFAR TEST SIMULATIONS

1.0 Rocket Input Tables (MK40, Mk151 WH)

1.1 Thrust-Impulse

burn time 1.551 sec
 ave. thrust 755 lb_f
 impulse 1171 lb_f-sec
 torque coefficient 0.002192 ft.
 est. burn curve: 8 pt. star, stabilizing rod: Thrust nearly constant

1.2 Mass Properties (length 50", dia. 2.75")

	mass (lb _m)	cg (tLf _{nose})	I ₁₁	I ₂₂ (slug-ft ²)
WH	10.00			
Motor	4.34			
Prop.	5.86			
Total (Loaded)	20.20	1.4896	0.17063	32.3403
Total (b.o.)	14.34	1.0521	0.13097	26.0208

1.3 Drag Coefficient ($A_{ref} = 0.04125 \text{ ft}^2$)

Mach	C _D
0.00	0.637
0.96	0.637
0.90	0.649
0.93	0.667
0.95	0.695
1.03	1.197
2.20	0.917

1.4 Normal Force Slope Coefficient

Mach	$C_{N\alpha}$
0.0000	13.9059
0.6000	13.9059
0.7000	12.7166
0.8000	13.4484
0.9000	13.4484
0.9500	13.1557
1.0000	14.2901
1.0500	14.2901
1.1000	13.8693
1.2000	12.9361
1.3000	12.2957
1.4000	11.1430
1.5000	11.1430
2.0000	9.1486
3.0000	8.9107
4.0000	8.9107
5.0000	8.8376

1.5 Center of Mass (ref. tail)

Time	CM (ft.)
0.000	2.677
1.551	3.115
2.500	3.115
999.000	3.115

1.6 Roll Moment of Inertia

Time	I_{11}
0.000	0.17063
1.551	0.13097
2.500	0.13097
999.000	0.13097

$$= c_d c_p c_{N\alpha}$$

hence:

$$c_d = \frac{Cm q d^2/2}{c_p c_{N\alpha}} = CPD$$

MACH	CMQ	CP	CNA	CPD
0.00	920	.5596	13.9059	3.1044
0.60	920	.5596	13.9059	3.1044
0.70	864	.5596	13.7166	3.1881
0.80	879	.6237	13.4484	2.7518
0.90	892	.6856	13.4484	2.5404
0.95	912	.5917	13.1557	3.0765
1.00	1039	.4977	14.2901	3.8361
1.05	1068	.4977	14.2901	3.9431
1.10	978	.5298	13.8693	3.4950
1.20	879	.5298	12.9361	3.4368
1.30	627	.7177	12.2957	1.8657
1.40	497	.7796	11.1430	1.5029
1.50	474	.8094	11.1430	1.3800
2.00	239	1.1233	9.1486	0.6107
3.00	131	1.3823	8.9107	0.2793

1.9 Center of Pressure (ref. nose, in calcs.)

Mach	C _p 0°	4°	12°	57.3
0.000	15.740	14.920	14.240	13.590
0.600	15.740	14.920	14.240	13.590
0.700	15.740	15.100	14.100	13.690
0.800	15.460	15.050	14.230	13.550
0.900	15.190	15.100	14.370	13.550
0.950	15.600	15.050	14.370	13.560
1.000	16.010	15.330	14.380	13.690
1.050	16.010	15.460	14.650	13.690

1.7 Pitch Moment of Inertia

Time	I_{22}
0.000	32.3403
1.551	26.0208
2.500	26.0208
999.000	26.0208

1.8 Pitch Damping Coefficient

Mach	C_{mq}
0.00	920
0.60	920
0.70	864
0.80	879
0.90	892
0.95	912
1.00	1039
1.05	1068
1.1	908
1.2	897
1.3	627
1.4	497
1.5	474
2.0	239
3.0	131

Transforming the damping coefficient

$$-qAC_{mq} d^2 \frac{\omega}{2V} = q AC_{N\alpha} [c_p (c_d - c_g) - c_g (c_p - c_g)]$$

about the tail:

$$C_{mq} d^2/2 = \sum_i C_{N\alpha i} r_i^2, \quad r_i = c_{pi} - c_g$$

1.100	15.870	15.190	14.370	13.420
1.200	15.870	14.920	14.240	13.140
1.300	15.050	14.640	14.100	13.140
1.400	14.780	14.370	13.690	13.000
1.500	14.650	14.370	13.690	12.730
2.000	13.280	13.280	13.280	12.440
3.000	12.150	12.150	12.150	12.150
4.000	11.480	11.480	11.480	11.480
5.000	10.965	10.965	10.965	10.965

Mach	C_p 0°	4°	8°	12°	57.3°
0.0000	0.5596	0.7475	0.9033	1.0523	1.0523
0.6000	0.5596	0.7475	0.9033	1.0523	1.0523
0.7000	0.5596	0.7062	0.9354	1.0294	1.0294
0.8000	0.6237	0.7177	0.9056	1.0614	1.0615
0.9000	0.6856	0.7062	0.8735	1.0615	1.0615
0.9500	0.5917	0.7177	0.8735	1.0592	1.0592
1.0000	0.4977	0.6535	0.8712	1.0294	1.0294
1.0500	0.4977	0.6237	0.8094	1.0294	1.0294
1.1000	0.5298	0.6856	0.8735	1.0912	1.0912
1.2000	0.5298	0.7475	0.9033	1.1554	1.1554
1.3000	0.7177	0.8117	0.9354	1.1554	1.1554
1.4000	0.7796	0.8735	1.0294	1.1875	1.1875
1.5000	0.8094	0.8735	1.0294	1.2494	1.2494
2.0000	1.1233	1.1233	1.1233	1.3158	1.3158
3.0000	1.3823	1.3823	1.3823	1.3823	1.3823
4.0000	1.5358	1.5358	1.5358	1.5358	1.5358
5.0000	1.6539	1.6539	1.6539	1.6539	1.6539

ref. "tail", in ft., "tail" 50 in. from nose.

1.10 Roll Damping Moment Coefficient

Mach	$C_{l\phi}$
0.0	14.770
1.0	14.770
2.0	14.770
5.0	14.770

DISTRIBUTION LIST

Dr. Frank D. Eaton
Geophysical Institute
University of Alaska
Fairbanks, AK 99701

Commander
US Army Aviation Center
ATTN: ATZQ-D-MA
Fort Rucker, AL 36362

Chief, Atmospheric Sciences Div
Code ES-81
NASA
Marshall Space Flight Center,
AL 35812

Commander
US Army Missile R&D Command
ATTN: DRDMI-CGA (B. W. Fowler)
Redstone Arsenal, AL 35809

Redstone Scientific Information Center
ATTN: DRDMI-TBD
US Army Missile R&D Command
Redstone Arsenal, AL 35809

Commander
US Army Missile R&D Command
ATTN: DRDMI-TEM (R. Haraway)
Redstone Arsenal, AL 35809

Commander
US Army Missile R&D Command
ATTN: DRDMI-TRA (Dr. Essenwanger)
Redstone Arsenal, AL 35809

Commander
HQ, Fort Huachuca
ATTN: Tech Ref Div
Fort Huachuca, AZ 85613

Commander
US Army Intelligence Center & School
ATTN: ATSI-CD-MD
Fort Huachuca, AZ 85613

Commander
US Army Yuma Proving Ground
ATTN: Technical Library
Bldg 2100
Yuma, AZ 85364

Naval Weapons Center (Code 3173)
ATTN: Dr. A. Shlanta
China Lake, CA 93555

Sylvania Elec Sys Western Div
ATTN: Technical Reports Library
PO Box 205
Mountain View, CA 94040

Geophysics Officer
PMTIC Code 3250
Pacific Missile Test Center
Point Mugu, CA 93042

Commander
Naval Ocean Systems Center (Code 4473)
ATTN: Technical Library
San Diego, CA 92152

Meteorologist in Charge
Kwajalein Missile Range
PO Box 67
APO San Francisco, CA 96555

Director
NOAA/ERL/APCL R31
RB3-Room 567
Boulder, CO 80302

Library-R-51-Tech Reports
NOAA/ERL
320 S. Broadway
Boulder, CO 80302

National Center for Atmos Research
NCAR Library
PO Box 3000
Boulder, CO 80307

R. B. Girardo
Bureau of Reclamation
E&R Center, Code 1220
Denver Federal Center, Bldg 67
Denver, CO 80225

National Weather Service
National Meteorological Center
W321, WWB, Room 201
ATTN: Mr. Quiroz
Washington, DC 20233

Mil Assistant for Atmos Sciences
Ofc of the Undersecretary of Defense
for Rsch & Engr/E&LS - Room 3D129
The Pentagon
Washington, DC 20301

Defense Communications Agency
Technical Library Center
Code 205
Washington, DC 20305

Director
Defense Nuclear Agency
ATTN: Technical Library
Washington, DC 20305

HQDA (DAEN-RDM/Dr. de Percin)
Washington, DC 20314

Director
Naval Research Laboratory
Code 5530
Washington, DC 20375

Commanding Officer
Naval Research Laboratory
Code 2627
Washington, DC 20375

Dr. J. M. MacCallum
Naval Research Laboratory
Code 1409
Washington, DC 20375

The Library of Congress
ATTN: Exchange & Gift Div
Washington, DC 20540
2

Head, Atmos Rsch Section
Div Atmospheric Science
National Science Foundation
1800 G. Street, NW
Washington, DC 20550

CPT Hugh Albers, Exec Sec
Interdept Committee on Atmos Science
National Science Foundation
Washington, DC 20550

Director, Systems R&D Service
Federal Aviation Administration
ATTN: ARD-54
2100 Second Street, SW
Washington, DC 20590

ADTC/DLODL
Eglin AFB, FL 32542

Naval Training Equipment Center
ATTN: Technical Library
Orlando, FL 32813

Det 11, 2WS/O1
ATTN: Maj Oronzorff
Patrick AFB, FL 32925

USAFETAC/CB
Scott AFB, IL 62225

HQ, ESD/TOSI/S-22
Hanscom AFB, MA 01731

Air Force Geophysics Laboratory
ATTN: LCB (A. S. Carten, Jr.)
Hanscom AFB, MA 01731

Air Force Geophysics Laboratory
ATTN: LYD
Hanscom AFB, MA 01731

Meteorology Division
AFGL/LY
Hanscom AFB, MA 01731

US Army Liaison Office
MIT-Lincoln Lab, Library A-082
PO Box 73
Lexington, MA 02173

Director
US Army Ballistic Rsch Lab
ATTN: DRDAR-BLB (Dr. G. E. Keller)
Aberdeen Proving Ground, MD 21005

Commander
US Army Ballistic Rsch Lab
ATTN: DRDAR-BLP
Aberdeen Proving Ground, MD 21005

Director
US Army Armament R&D Command
Chemical Systems Laboratory
ATTN: DRDAR-CLJ-I
Aberdeen Proving Ground, MD 21010

Chief CB Detection & Alarms Div
Chemical Systems Laboratory
ATTN: DRDAR-CLC-CR (H. Tannenbaum)
Aberdeen Proving Ground, MD 21010

Commander
Harry Diamond Laboratories
ATTN: DELHD-CO
2800 Powder Mill Road
Adelphi, MD 20783

Commander
ERADCOM
ATTN: DRDEL-AP
2800 Powder Mill Road
Adelphi, MD 20783
2

Commander
ERADCOM
ATTN: DRDEL-CG/DRDEL-DC/DRDEL-CS
2800 Powder Mill Road
Adelphi, MD 20783

Commander
ERADCOM
ATTN: DRDEL-CT
2800 Powder Mill Road
Adelphi, MD 20783

Commander
ERADCOM
ATTN: DRDEL-EA
2800 Powder Mill Road
Adelphi, MD 20783

Commander
ERADCOM
ATTN: DRDEL-PA/DRDEL-ILS/DRDEL-E
2800 Powder Mill Road
Adelphi, MD 20783

Commander
ERADCOM
ATTN: DRDEL-PAO (S. Kimmel)
2800 Powder Mill Road
Adelphi, MD 20783

Chief
Intelligence Materiel Dev & Support Ofc
ATTN: DELEW-WL-I
Bldg 4554
Fort George G. Meade, MD 20755

Acquisitions Section, IRDB-D823
Library & Info Service Div, NOAA
6009 Executive Blvd
Rockville, MD 20852

Naval Surface Weapons Center
White Oak Library
Silver Spring, MD 20910

The Environmental Research
Institute of MI
ATTN: IRIA Library
PO Box 8618
Ann Arbor, MI 48107

Mr. William A. Main
USDA Forest Service
1407 S. Harrison Road
East Lansing, MI 48823

Dr. A. D. Belmont
Research Division
PO Box 1249
Control Data Corp
Minneapolis, MN 55440

Director
Naval Oceanography & Meteorology
NSTL Station
Bay St Louis, MS 39529

Director
US Army Engr Waterways Experiment Sta
ATTN: Library
PO Box 631
Vicksburg, MS 39180

Environmental Protection Agency
Meteorology Laboratory
Research Triangle Park, NC 27711

US Army Research Office
ATTN: DRXRO-PP
PO Box 12211
Research Triangle Park, NC 27709

Commanding Officer
US Army Armament R&D Command
ATTN: DRDAR-TSS Bldg 59
Dover, NJ 07801

Commander
HQ, US Army Avionics R&D Activity
ATTN: DAVAA-0
Fort Monmouth, NJ 07703

Commander/Director
US Army Combat Surveillance & Target
Acquisition Laboratory
ATTN: DELCS-D
Fort Monmouth, NJ 07703

Commander
US Army Electronics R&D Command
ATTN: DELCS-S
Fort Monmouth, NJ 07703

US Army Materiel Systems
Analysis Activity
ATTN: DRXSY-MP
Aberdeen Proving Ground, MD 21005

Director
US Army Electronics Technology &
Devices Laboratory
ATTN: DELET-D
Fort Monmouth, NJ 07703

Commander
US Army Electronic Warfare Laboratory
ATTN: DELEW-D
Fort Monmouth, NJ 07703

Commander
US Army Night Vision &
Electro-Optics Laboratory
ATTN: DELNV-L (Dr. Rudolf Buser)
Fort Monmouth, NJ 07703

Commander
ERADCOM Technical Support Activity
ATTN: DELSD-L
Fort Monmouth, NJ 07703

Project Manager, FIREFINDER
ATTN: DRCPM-FF
Fort Monmouth, NJ 07703

Project Manager, REMBASS
ATTN: DRCPM-RBS
Fort Monmouth, NJ 07703

Commander
US Army Satellite Comm Agency
ATTN: DRCPM-SC-3
Fort Monmouth, NJ 07703

Commander
ERADCOM Scientific Advisor
ATTN: DRDEL-SA
Fort Monmouth, NJ 07703

6585 TG/WE
Holloman AFB, NM 88330

AFWL/WE
Kirtland, AFB, NM 87117

AFWL/Technical Library (SUL)
Kirtland AFB, NM 87117

Commander
US Army Test & Evaluation Command
ATTN: STEWS-AD-L
White Sands Missile Range, NM 88002

Rome Air Development Center
ATTN: Documents Library
TSLD (Bette Smith)
Griffiss AFB, NY 13441

Commander
US Army Tropic Test Center
ATTN: STETC-TD (Info Center)
APO New York 09827

Commandant
US Army Field Artillery School
ATTN: ATSF-CD-R (Mr. Farmer)
Fort Sill, OK 73503

Commandant
US Army Field Artillery School
ATTN: ATSF-CF-R
Fort Sill, OK 73503

Director CFD
US Army Field Artillery School
ATTN: Met Division
Fort Sill, OK 73503

Commandant
US Army Field Artillery School
ATTN: Morris Swett Library
Fort Sill, OK 73503

Commander
US Army Dugway Proving Ground
ATTN: MT-DA-L
Dugway, UT 84022

Dr. C. R. Sreedrahan
Research Associates
Utah State University, UNC 48
Logan, UT 84322

Inge Dirmhirn, Professor
Utah State University, UNC 48
Logan, UT 84322

Defense Documentation Center
ATTN: DDC-TCA
Cameron Station Bldg 5
Alexandria, VA 22314
12

Commanding Officer
US Army Foreign Sci & Tech Center
ATTN: DRXST-IS1
220 7th Street, NE
Charlottesville, VA 22901

Naval Surface Weapons Center
Code G65
Dahlgren, VA 22448

Commander
US Army Night Vision
& Electro-Optics Lab
ATTN: DELNV-D
Fort Belvoir, VA 22060

Commander and Director
US Army Engineer Topographic Lab
ETL-TD-MB
Fort Belvoir, VA 22060

Director
Applied Technology Lab
DAVDL-EU-TSD
ATTN: Technical Library
Fort Eustis, VA 23604

Department of the Air Force
OL-C, 5WW
Fort Monroe, VA 23651

Department of the Air Force
5WW/DN
Langley AFB, VA 23665

Director
Development Center MCDEC
ATTN: Firepower Division
Quantico, VA 22134

US Army Nuclear & Chemical Agency
ATTN: MONA-WE
Springfield, VA 22150

Director
US Army Signals Warfare Laboratory
ATTN: DELSW-OS (Dr. R. Burkhardt)
Vint Hill Farms Station
Warrenton, VA 22186

Commander
US Army Cold Regions Test Center
ATTN: STECR-OP-PM
APO Seattle, WA 98733

Dr. John L. Walsh
Code 5560
Navy Research Lab
Washington, DC 20375

Commander
TRASANA
ATTN: ATAA-PL
(Dolores Anguiano)
White Sands Missile Range, NM 88002

Commander
US Army Dugway Proving Ground
ATTN: STEDP-MT-DA-M (Mr. Paul Carlson)
Dugway, UT 84022

Commander
US Army Dugway Proving Ground
ATTN: STEDP-MT-DA-T
(Mr. William Peterson)
Dugway, UT 84022

Commander
USATRADO
ATTN: ATCD-SIE
Fort Monroe, VA 23651

Commander
USATRADO
ATTN: ATCD-CF
Fort Monroe, VA 23651

Commander
USATRADO
ATTN: Tech Library
Fort Monroe, VA 23651

ATMOSPHERIC SCIENCES RESEARCH PAPERS

1. Lindberg, J.D., "An Improvement to a Method for Measuring the Absorption Coefficient of Atmospheric Dust and other Strongly Absorbing Powders," ECOM-5565, July 1975.
2. Avara, Elton, P., "Mesoscale Wind Shears Derived from Thermal Winds," ECOM-5566, July 1975.
3. Gomez, Richard B., and Joseph H. Pierluissi, "Incomplete Gamma Function Approximation for King's Strong-Line Transmittance Model," ECOM-5567, July 1975.
4. Blanco, A.J., and B.F. Engebos, "Ballistic Wind Weighting Functions for Tank Projectiles," ECOM-5568, August 1975.
5. Taylor, Fredrick J., Jack Smith, and Thomas H. Pries, "Crosswind Measurements through Pattern Recognition Techniques," ECOM-5569, July 1975.
6. Walters, D.L., "Crosswind Weighting Functions for Direct-Fire Projectiles," ECOM-5570, August 1975.
7. Duncan, Louis D., "An Improved Algorithm for the Iterated Minimal Information Solution for Remote Sounding of Temperature," ECOM-5571, August 1975.
8. Robbiani, Raymond L., "Tactical Field Demonstration of Mobile Weather Radar Set AN/TPS-41 at Fort Rucker, Alabama," ECOM-5572, August 1975.
9. Miers, B., G. Blackman, D. Langer, and N. Lorimier, "Analysis of SMS/GOES Film Data," ECOM-5573, September 1975.
10. Manquero, Carlos, Louis Duncan, and Rufus Bruce, "An Indication from Satellite Measurements of Atmospheric CO₂ Variability," ECOM-5574, September 1975.
11. Petracca, Carmine, and James D. Lindberg, "Installation and Operation of an Atmospheric Particulate Collector," ECOM-5575, September 1975.
12. Avara, Elton P., and George Alexander, "Empirical Investigation of Three Iterative Methods for Inverting the Radiative Transfer Equation," ECOM-5576, October 1975.
13. Alexander, George D., "A Digital Data Acquisition Interface for the SMS Direct Readout Ground Station — Concept and Preliminary Design," ECOM-5577, October 1975.
14. Cantor, Israel, "Enhancement of Point Source Thermal Radiation Under Clouds in a Nonattenuating Medium," ECOM-5578, October 1975.
15. Norton, Colburn, and Glenn Hoidale, "The Diurnal Variation of Mixing Height by Month over White Sands Missile Range, N.M.," ECOM-5579, November 1975.
16. Avara, Elton P., "On the Spectrum Analysis of Binary Data," ECOM-5580, November 1975.
17. Taylor, Fredrick J., Thomas H. Pries, and Chao-Huan Huang, "Optimal Wind Velocity Estimation," ECOM-5581, December 1975.
18. Avara, Elton P., "Some Effects of Autocorrelated and Cross-Correlated Noise on the Analysis of Variance," ECOM-5582, December 1975.
19. Gillespie, Patti S., R.L. Armstrong, and Kenneth O. White, "The Spectral Characteristics and Atmospheric CO₂ Absorption of the Ho³⁺YLF Laser at 2.05 μ m," ECOM-5583, December 1975.
20. Novlan, David J., "An Empirical Method of Forecasting Thunderstorms for the White Sands Missile Range," ECOM-5584, February 1976.
21. Avara, Elton P., "Randomization Effects in Hypothesis Testing with Autocorrelated Noise," ECOM-5585, February 1976.
22. Watkins, Wendell R., "Improvements in Long Path Absorption Cell Measurement," ECOM-5586, March 1976.
23. Thomas, Joe, George D. Alexander, and Marvin Dubbin, "SATTEL — An Army Dedicated Meteorological Telemetry System," ECOM-5587, March 1976.
24. Kennedy, Bruce W., and Delbert Bynum, "Army User Test Program for the RDT&E-XM-75 Meteorological Rocket," ECOM-5588, April 1976.

25. Barnett, Kenneth M., "A Description of the Artillery Meteorological Comparisons at White Sands Missile Range, October 1974 - December 1974 ('PASS' - Prototype Artillery [Meteorological] Subsystem)," ECOM-5589, April 1976.
26. Miller, Walter B., "Preliminary Analysis of Fall-of-Shot From Project 'PASS'," ECOM-5590, April 1976.
27. Avara, Elton P., "Error Analysis of Minimum Information and Smith's Direct Methods for Inverting the Radiative Transfer Equation," ECOM-5591, April 1976.
28. Yee, Young P., James D. Horn, and George Alexander, "Synoptic Thermal Wind Calculations from Radiosonde Observations Over the Southwestern United States," ECOM-5592, May 1976.
29. Duncan, Louis D., and Mary Ann Seagraves, "Applications of Empirical Corrections to NOAA-4 VTPR Observations," ECOM-5593, May 1976.
30. Miers, Bruce T., and Steve Weaver, "Applications of Meteorological Satellite Data to Weather Sensitive Army Operations," ECOM-5594, May 1976.
31. Sharenow, Moses, "Redesign and Improvement of Balloon ML-566," ECOM-5595, June, 1976.
32. Hansen, Frank V., "The Depth of the Surface Boundary Layer," ECOM-5596, June 1976.
33. Pinnick, R.G., and E.B. Stenmark, "Response Calculations for a Commercial Light-Scattering Aerosol Counter," ECOM-5597, July 1976.
34. Mason, J., and G.B. Hoidale, "Visibility as an Estimator of Infrared Transmittance," ECOM-5598, July 1976.
35. Bruce, Rufus E., Louis D. Duncan, and Joseph H. Pierluissi, "Experimental Study of the Relationship Between Radiosonde Temperatures and Radiometric-Area Temperatures," ECOM-5599, August 1976.
36. Duncan, Louis D., "Stratospheric Wind Shear Computed from Satellite Thermal Sounder Measurements," ECOM-5800, September 1976.
37. Taylor, F., P. Mohan, P. Joseph and T. Pries, "An All Digital Automated Wind Measurement System," ECOM-5801, September 1976.
38. Bruce, Charles, "Development of Spectrophones for CW and Pulsed Radiation Sources," ECOM-5802, September 1976.
39. Duncan, Louis D., and Mary Ann Seagraves, "Another Method for Estimating Clear Column Radiances," ECOM-5803, October 1976.
40. Blanco, Abel J., and Larry E. Taylor, "Artillery Meteorological Analysis of Project Pass," ECOM-5804, October 1976.
41. Miller, Walter, and Bernard Engebos, "A Mathematical Structure for Refinement of Sound Ranging Estimates," ECOM-5805, November, 1976.
42. Gillespie, James B., and James D. Lindberg, "A Method to Obtain Diffuse Reflectance Measurements from 1.0 to 3.0 μm Using a Cary 171 Spectrophotometer," ECOM-5806, November 1976.
43. Rubio, Roberto, and Robert O. Olsen, "A Study of the Effects of Temperature Variations on Radio Wave Absorption," ECOM-5807, November 1976.
44. Ballard, Harold N., "Temperature Measurements in the Stratosphere from Balloon-Borne Instrument Platforms, 1968-1975," ECOM-5808, December 1976.
45. Monahan, H.H., "An Approach to the Short-Range Prediction of Early Morning Radiation Fog," ECOM-5809, January 1977.
46. Engebos, Bernard Francis, "Introduction to Multiple State Multiple Action Decision Theory and Its Relation to Mixing Structures," ECOM-5810, January 1977.
47. Low, Richard D.H., "Effects of Cloud Particles on Remote Sensing from Space in the 10-Micrometer Infrared Region," ECOM-5811, January 1977.
48. Bonner, Robert S., and R. Newton, "Application of the AN/GVS-5 Laser Rangefinder to Cloud Base Height Measurements," ECOM-5812, February 1977.
49. Rubio, Roberto, "Lidar Detection of Subvisible Reentry Vehicle Erosive Atmospheric Material," ECOM-5813, March 1977.
50. Low, Richard D.H., and J.D. Horn, "Mesoscale Determination of Cloud-Top Height: Problems and Solutions," ECOM-5814, March 1977.

51. Duncan, Louis D., and Mary Ann Seagraves, "Evaluation of the NOAA-4 VTPR Thermal Winds for Nuclear Fallout Predictions," ECOM-5815, March 1977.
52. Randhawa, Jagir S., M. Izquierdo, Carlos McDonald and Zvi Salpeter, "Stratospheric Ozone Density as Measured by a Chemiluminescent Sensor During the Stratcom VI-A Flight," ECOM-5816, April 1977.
53. Rubio, Roberto, and Mike Izquierdo, "Measurements of Net Atmospheric Irradiance in the 0.7- to 2.8-Micrometer Infrared Region," ECOM-5817, May 1977.
54. Ballard, Harold N., Jose M. Serna, and Frank P. Hudson Consultant for Chemical Kinetics, "Calculation of Selected Atmospheric Composition Parameters for the Mid-Latitude, September Stratosphere," ECOM-5818, May 1977.
55. Mitchell, J.D., R.S. Sagar, and R.O. Olsen, "Positive Ions in the Middle Atmosphere During Sunrise Conditions," ECOM-5819, May 1977.
56. White, Kenneth O., Wendell R. Watkins, Stuart A. Schleusener, and Ronald L. Johnson, "Solid-State Laser Wavelength Identification Using a Reference Absorber," ECOM-5820, June 1977.
57. Watkins, Wendell R., and Richard G. Dixon, "Automation of Long-Path Absorption Cell Measurements," ECOM-5821, June 1977.
58. Taylor, S.E., J.M. Davis, and J.B. Mason, "Analysis of Observed Soil Skin Moisture Effects on Reflectance," ECOM-5822, June 1977.
59. Duncan, Louis D. and Mary Ann Seagraves, "Fallout Predictions Computed from Satellite Derived Winds," ECOM-5823, June 1977.
60. Snider, D.E., D.G. Murcray, F.H. Murcray, and W.J. Williams, "Investigation of High-Altitude Enhanced Infrared Background Emissions" (U), SECRET, ECOM-5824, June 1977.
61. Dubbin, Marvin H. and Dennis Hall, "Synchronous Meteorological Satellite Direct Readout Ground System Digital Video Electronics," ECOM-5825, June 1977.
62. Miller, W., and B. Engebos, "A Preliminary Analysis of Two Sound Ranging Algorithms," ECOM-5826, July 1977.
63. Kennedy, Bruce W., and James K. Luers, "Ballistic Sphere Techniques for Measuring Atmospheric Parameters," ECOM-5827, July 1977.
64. Duncan, Louis D., "Zenith Angle Variation of Satellite Thermal Sounder Measurements," ECOM-5828, August 1977.
65. Hansen, Frank V., "The Critical Richardson Number," ECOM-5829, September 1977.
66. Ballard, Harold N., and Frank P. Hudson (Compilers), "Stratospheric Composition Balloon-Borne Experiment," ECOM-5830, October 1977.
67. Barr, William C., and Arnold C. Peterson, "Wind Measuring Accuracy Test of Meteorological Systems," ECOM-5831, November 1977.
68. Ethridge, G.A. and F.V. Hansen, "Atmospheric Diffusion: Similarity Theory and Empirical Derivations for Use in Boundary Layer Diffusion Problems," ECOM-5832, November 1977.
69. Low, Richard D.H., "The Internal Cloud Radiation Field and a Technique for Determining Cloud Blackness," ECOM-5833, December 1977.
70. Watkins, Wendell R., Kenneth O. White, Charles W. Bruce, Donald L. Walters, and James D. Lindberg, "Measurements Required for Prediction of High Energy Laser Transmission," ECOM-5834, December 1977.
71. Rubio, Robert, "Investigation of Abrupt Decreases in Atmospherically Backscattered Laser Energy," ECOM-5835, December 1977.
72. Monahan, H.H. and R.M. Cionco, "An Interpretative Review of Existing Capabilities for Measuring and Forecasting Selected Weather Variables (Emphasizing Remote Means)," ASL-TR-0001, January 1978.
73. Heaps, Melvin G., "The 1979 Solar Eclipse and Validation of D-Region Models," ASL-TR-0002, March 1978.

74. Jennings, S.G., and J.B. Gillespie, "M.I.E. Theory Sensitivity Studies - The Effects of Aerosol Complex Refractive Index and Size Distribution Variations on Extinction and Absorption Coefficients Part II: Analysis of the Computational Results," ASL-TR-0003, March 1978.
75. White, Kenneth O. et al, "Water Vapor Continuum Absorption in the 3.5 μ m to 4.0 μ m Region," ASL-TR-0004, March 1978.
76. Olsen, Robert O., and Bruce W. Kennedy, "ABRES Pretest Atmospheric Measurements," ASL-TR-0005, April 1978.
77. Ballard, Harold N., Jose M. Serna, and Frank P. Hudson, "Calculation of Atmospheric Composition in the High Latitude September Stratosphere," ASL-TR-0006, May 1978.
78. Watkins, Wendell R. et al, "Water Vapor Absorption Coefficients at HF Laser Wavelengths," ASL-TR-0007, May 1978.
79. Hansen, Frank V., "The Growth and Prediction of Nocturnal Inversions," ASL-TR-0008, May 1978.
80. Samuel, Christine, Charles Bruce, and Ralph Brewer, "Spectrophone Analysis of Gas Samples Obtained at Field Site," ASL-TR-0009, June 1978.
81. Pinnick, R.G. et al., "Vertical Structure in Atmospheric Fog and Haze and its Effects on IR Extinction," ASL-TR-0010, July 1978.
82. Low, Richard D.H., Louis D. Duncan, and Richard B. Gomez, "The Microphysical Basis of Fog Optical Characterization," ASL-TR-0011, August 1978.
83. Heaps, Melvin G., "The Effect of a Solar Proton Event on the Minor Neutral Constituents of the Summer Polar Mesosphere," ASL-TR-0012, August 1978.
84. Mason, James B., "Light Attenuation in Falling Snow," ASL-TR-0013, August 1978.
85. Blanco, Abel J., "Long-Range Artillery Sound Ranging: "PASS" Meteorological Application," ASL-TR-0014, September 1978.
86. Heaps, M.G., and F.E. Niles, "Modeling the Ion Chemistry of the D-Region: A case Study Based Upon the 1966 Total Solar Eclipse," ASL-TR-0015, September 1978.
87. Jennings, S.G., and R.G. Pinnick, "Effects of Particulate Complex Refractive Index and Particle Size Distribution Variations on Atmospheric Extinction and Absorption for Visible Through Middle-Infrared Wavelengths," ASL-TR-0016, September 1978.
88. Watkins, Wendell R., Kenneth O. White, Lanny R. Bower, and Brian Z. Sojka, "Pressure Dependence of the Water Vapor Continuum Absorption in the 3.5- to 4.0-Micrometer Region," ASL-TR-0017, September 1978.
89. Miller, W.B., and B.F. Engebos, "Behavior of Four Sound Ranging Techniques in an Idealized Physical Environment," ASL-TR-0018, September 1978.
90. Gomez, Richard G., "Effectiveness Studies of the CBU-88/B Bomb, Cluster, Smoke Weapon" (U), CONFIDENTIAL ASL-TR-0019, September 1978.
91. Miller, August, Richard C. Shirkey, and Mary Ann Seagraves, "Calculation of Thermal Emission from Aerosols Using the Doubling Technique," ASL-TR-0020, November, 1978.
92. Lindberg, James D. et al., "Measured Effects of Battlefield Dust and Smoke on Visible, Infrared, and Millimeter Wavelengths Propagation: A Preliminary Report on Dusty Infrared Test-I (DIRT-I)," ASL-TR-0021, January 1979.
93. Kennedy, Bruce W., Arthur Kinghorn, and B.R. Hixon, "Engineering Flight Tests of Range Meteorological Sounding System Radiosonde," ASL-TR-0022, February 1979.
94. Rubio, Roberto, and Don Hooek, "Microwave Effective Earth Radius Factor Variability at Wiesbaden and Balboa," ASL-TR-0023, February 1979.
95. Low, Richard D.H., "A Theoretical Investigation of Cloud/Fog Optical Properties and Their Spectral Correlations," ASL-TR-0024, February 1979.

96. Pinnick, R.G., and H.J. Auvermann, "Response Characteristics of Knollenberg Light-Scattering Aerosol Counters," ASL-TR-0025, February 1979.
97. Heaps, Melvin G., Robert O. Olsen, and Warren W. Berning, "Solar Eclipse 1979, Atmospheric Sciences Laboratory Program Overview," ASL-TR-0026 February 1979.
98. Blanco, Abel J., "Long-Range Artillery Sound Ranging: 'PASS' GR-8 Sound Ranging Data," ASL-TR-0027, March 1979.
99. Kennedy, Bruce W., and Jose M. Serna, "Meteorological Rocket Network System Reliability," ASL-TR-0028, March 1979.
100. Swingle, Donald M., "Effects of Arrival Time Errors in Weighted Range Equation Solutions for Linear Base Sound Ranging," ASL-TR-0029, April 1979.
101. Umstead, Robert K., Ricardo Pena, and Frank V. Hansen, "KWIK: An Algorithm for Calculating Munition Expenditures for Smoke Screening/Obscuration in Tactical Situations," ASL-TR-0030, April 1979.
102. D'Arcy, Edward M., "Accuracy Validation of the Modified Nike Hercules Radar," ASL-TR-0031, May 1979.
103. Rodriguez, Ruben, "Evaluation of the Passive Remote Crosswind Sensor," ASL-TR-0032, May 1979.
104. Barber, T.L., and R. Rodriguez, "Transit Time Lidar Measurement of Near-Surface Winds in the Atmosphere," ASL-TR-0033, May 1979.
105. Low, Richard D.H., Louis D. Duncan, and Y.Y. Roger R. Hsiao, "Microphysical and Optical Properties of California Coastal Fogs at Fort Ord," ASL-TR-0034, June 1979.
106. Rodriguez, Ruben, and William J. Vechione, "Evaluation of the Saturation Resistant Crosswind Sensor," ASL-TR-0035, July 1979.
107. Ohmstede, William D., "The Dynamics of Material Layers," ASL-TR-0036, July 1979.
108. Pinnick, R.G., S.G. Jennings, Petr Chylek, and H.J. Auvermann "Relationships between IR Extinction, Absorption, and Liquid Water Content of Fogs," ASL-TR-0037, August 1979.
109. Rodriguez, Ruben, and William J. Vechione, "Performance Evaluation of the Optical Crosswind Profiler," ASL-TR-0038, August 1979.
110. Miers, Bruce T., "Precipitation Estimation Using Satellite Data" ASL-TR-0039, September 1979.
111. Dickson, David H., and Charles M. Sonnenschein, "Helicopter Remote Wind Sensor System Description," ASL-TR-0040, September 1979.
112. Heaps, Melvin, G., and Joseph M. Heimerl, "Validation of the Dairchem Code, I: Quiet Midlatitude Conditions," ASL-TR-0041, September 1979.
113. Bonner, Robert S., and William J. Lentz, "The Visioceilometer: A Portable Cloud Height and Visibility Indicator," ASL-TR-0042, October 1979.
114. Cohn, Stephen L., "The Role of Atmospheric Sulfates in Battlefield Obscurations," ASL-TR-0043, October 1979.
115. Fawbush, E.J. et al, "Characterization of Atmospheric Conditions at the High Energy Laser System Test Facility (HELSTF), White Sands Missile Range, New Mexico, Part I, 24 March to 8 April 1977," ASL-TR-0044, November 1979.
116. Barber, Ted L., "Short-Time Mass Variation in Natural Atmospheric Dust," ASL-TR-0045, November 1979.
117. Low, Richard D.H., "Fog Evolution in the Visible and Infrared Spectral Regions and its Meaning in Optical Modeling," ASL-TR-0046, December 1979.
118. Duncan, Louis D. et al, "The Electro-Optical Systems Atmospheric Effects Library, Volume I: Technical Documentation, ASL-TR-0047, December 1979.
119. Shirkey, R. C. et al, "Interim E-O SAEL, Volume II, Users Manual," ASL-TR-0048, December 1979.
120. Kobayashi, H.K., "Atmospheric Effects on Millimeter Radio Waves," ASL-TR-0049, January 1980.
121. Seagraves, Mary Ann and Duncan, Louis D., "An Analysis of Transmittances Measured Through Battlefield Dust Clouds," ASL-TR-0050, February, 1980.

122. Dickson, David H., and Jon E. Ottesen, "Helicopter Remote Wind Sensor Flight Test,"
ASL-TR-0051, February 1980.